# ANALYSIS OF VIVALDI ANTENNA

*By*

N. SRIKANTH SHARMA



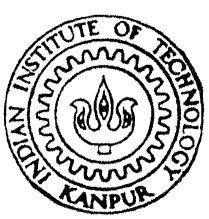


DEPARTMENT OF ELECTRICAL ENGINEERING

INDIAN INSTITUTE OF TECHNOLOGY KANPUR

MAY, 1991

# ANALYSIS OF VIVALDI ANTENNA

*A Thesis Submitted*
*in Partial Fulfilment of the Requirements*
*for the Degree of*
*MASTER OF TECHNOLOGY*

*By*
N. SRIKANTH SHARMA

to the
DEPARTMENT OF ELECTRICAL ENGINEERING
**INDIAN INSTITUTE OF TECHNOLOGY KANPUR**
MAY, 1991

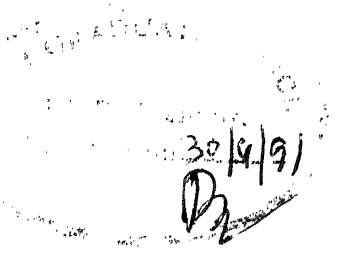

# CERTIFICATE

Certified that the thesis entitled, "ANALYSIS OF VIVALDI ANTENNA" by N. Srikanth Sharma has been carried out under my supervision and the same has not been submitted elsewhere for a degree.

(M. Sachidananda)
Assistant Professor
Electrical Engineering Dept.
Indian Instiltute of Technology
Kanpur 208 016

April 30, 1991

# ABSTRACT

This thesis presents an analysis of a vivaldi antenna. It is a broad band antenna realised in a printed form. The most commonly used numerical technique. "The moment method" is discussed. Its implementation is explained by applying it to some simple structures like a dipole and a rectangular microstrip antenna. An IBM-PC compatible A-D card is fabricated and used to measure the approximate form of current distribution on the antenna. The theory of the sampling probe is presented. Finally the antenna is made to fit in an elliptic cylinder coordinate system and approximate form of bases functions given based on the experimental results.

# ACKNOWLEDGEMENTS

I express my deep sense of gratitude to my thesis supervisor Dr. M. Sachidananda for actively participating at each level with invaluable guidance and encouragement without which the work would not have been possible.

I am grateful to Dr. R. Sharan, Dr. K.R. Srivathsan, Dr. M.S. Tyagi and Dr. M.M. Hasan for having taught me wonderful things.

I thank K. Muralikrishna for having helped me during my thesis. I am thankful to R. Hari Prasad, Venugopal, Ramesh, Sita Ram, Srinivas Rao, Inderjit and Subba Rao due to whom I had a delightful stay at IIT.

(Srikanth Sharma)

# CONTENTS


| hapter | | Page |
|---|---|---|
| I. | INTRODUCTION | 1 |
| | 1.1 Introduction | |
| | 1.2 Literature Survey | |
| | 1.3 Aim of the Present Work | |
| II. | MOMENT METHOD | 6 |
| | 2.1 Introduction | |
| | 2.2 Formulation of the Integral Equation | |
| | 2.3 The Moment Method | |
| | 2.4 Moment Method as Applied to a Dipole | |
| | 2.5 Moment Method as Applied to Microstrip Antennas | |
| III. | MEASUREMENT OF CURRENT DISTRIBUTION ON VIVALDI ANTENNA | 35 |
| | 3.1 Introduction | |
| | 3.2 Experimental Measurement of Current Distribution | |
| | 3.3 Sampling Probe-Theory and Design | |
| | 3.4 Design of A-D Card | |
| | 3.5 Measurement | |
| | 3.6 Results and Discussion | |
| IV. | VIVALDI ANTENNA IN ELLIPTIC CYLINDER COORDINATES | 60 |
| | 4.1 Introduction | |
| | 4.2 Elliptic-Cylinder Coordinates | |
| | 4.3 Entire Domain Functions | |
| | 4.4 Expression for Near-Field Evaluation | |
| V. | SUMMARY, CONCLUSION AND SCOPE FOR FURTHER WORK | 70 |
| | 5.1 Summary and Conclusions | |
| | 5.2 Scope for Further Work | |
| | REFERENCES | 72 |
| | APPENDIX 1 | 74 |
| | APPENDIX 2 | 76 |

# CHAPTER I

# INTRODUCTION

## INTRODUCTION

The developments in the field of antennas have come a long way through from the conventional antennas like dish antenna, yagiuda antenna etc. to the modern microstrip antennas. With the advent of high speed computers and new mathematical tools to solve the difficult electromagnetic equations numerically, the antenna field has taken a great stride. The advantages of microstrip antennas being numerous like light weight, low cost, easy reproducibility etc. [1] all the applications of conventional antennas are being tried to be handled by the patch antennas. One such innovative step is the realisation of broad band antennas in printed form. All the microstrip planar antennas are of the form which has a resonant cavity and hence a low bandwidth, but the introduction of vivaldi antenna by Gibson et.al. [2] has led to the use of printed antennas in broadband applications.

## LITERATURE SURVEY:

Until the introduction of Vivaldi antenna by Gibson [2] and end fire tapered slot antenna by Mahapatra and Prasad [3] there was no well known planar antenna which could produce a well

defined end fire beam with appreciable bandwidth. Gibson [2] showed that the vivaldi antenna is capable of producing symmetric beam over a wide band width (3:1). His antenna consisted of metallized dielectric substrate with an exponential slot in the metallization. This type of antenna is capable of multi-active bandwidth. The length and operative size of such an antenna are determined by the lowest frequency of operation. At the lowest frequency length has to be greater than wavelength, and the operative size of about half wavelength for efficient radiation.

R.K. Janaswamy [4] has analysed the antenna to calculate the radiation pattern by assuming it to be approxximated by a stepped slot line. The geometry of the antenna and the approximation are as shows in the Fig. [ 1 ].

But this method was valid only for antenna whose operative size is small. His method of analysis consisted of two steps. In the first step, the tangential component of the electric-field distribution in the tapered slot, is obtained. In the second step, far fields radiated by the equivalent magnetic current in the slot are obtained using an appropriate Green's function.

The aperture distribution in the tapered slot is determined by employing the usual travelling wave antenna assumption that the aperture distribution is governed predominantly by the propogating modes. He divides the antenna into a number of sections of line of uniform width connected end to end. Then use is made of the theory of small reflections to get an overall reflection coefficient.

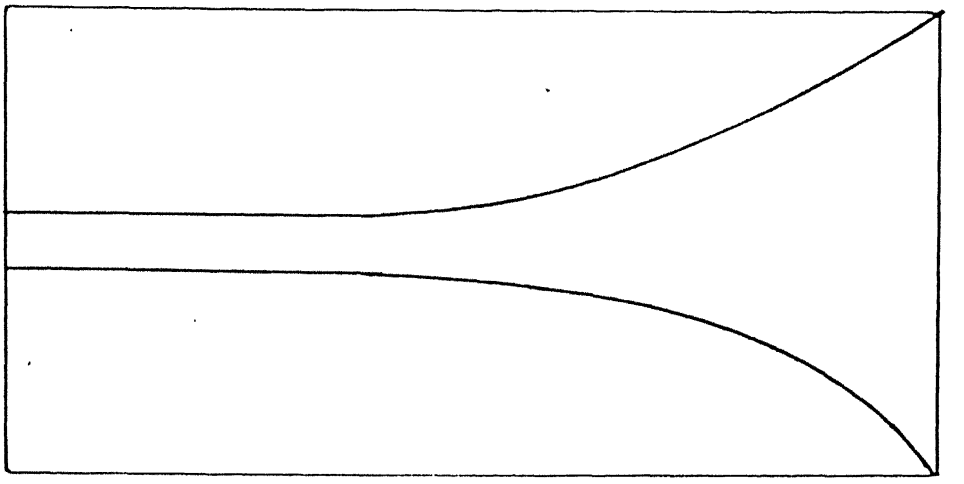

A. Exponential slot line

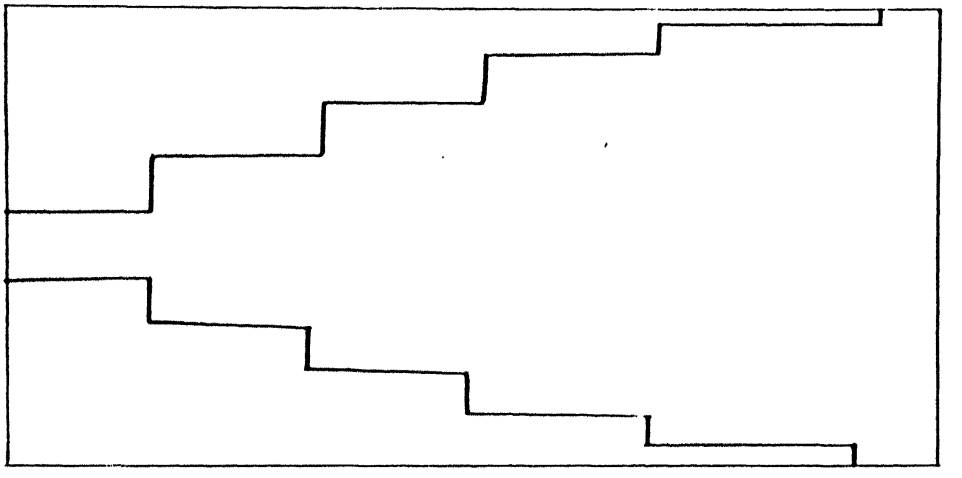

B.

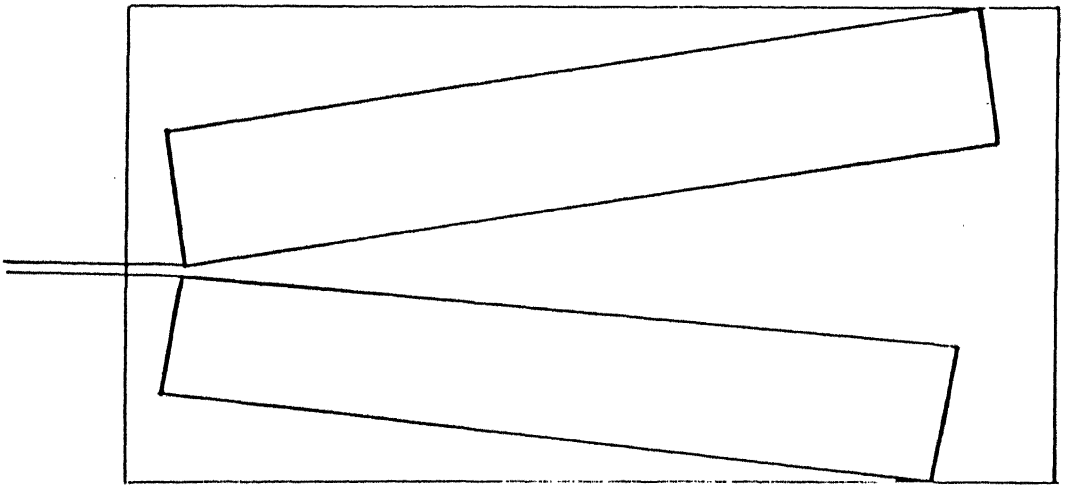

Fig 1 C. Geometries as solved in [4] and [5]

Later the same author [5] solved the antenna by approximating it as shown in Fig. [ 1 ].

The solution was based on the Moment Method Solution of the electric field Integral equation for the electric surface currents flowing on the conducting plates of the antenna. The geometry is such that use can be made of simple rectangular patches in the Moment Method Solution. The presence of the dielectric is included in the Moment Method Solution via the impedance boundary conditions. The current distribution and Input Impedance were calculated. The method is valid for arbitrary aperture widths.

S.N. Prasad and Mahapatra [3] gave the experimental results of a slot line antenna that operates in X-band with a gain of 6 dB and a side lobe level of 10 dB.

Ehid Gazit [6] gives a novel method of feeding the vivaldi antenna. He explains about the effects of transition from miscrostrip line to asymmetric slot line, and the effect it has on the band width characteristics.

The various attempts to solve the vivaldi antenna had moment method formulation using Subdomain functions. The use of Subdomain functions has the disadvantage of taking a lot of computer time. Even the use of surface patch dipoles as subdomain functions took a time of 8 to 10 hours [5]. Also the shape of the vivaldi antenna is such that ordinary subdomain functions like rectangular or triangular patches cannot be used to represent the antenna completely. The approximations which

have to be made in the shape of the antenna are many due to which the analysed antenna cannot truly represent the actual vivaldi antenna.

AIM OF THE PRESENT WORK:

Keeping in view the difficulties involved in the analysis of the vivaldi antenna, an effort is made to find the reasons for the drawbacks involved, the complexities of the moment method and an attempt to solve it in a different fashion.

In Chapter II the design details of the antenna, the feed of the antenna and other particulars discussed. The formulation of the Integral equation and the most commonly used numerical technique, the moment method are also discussed. The moment method is applied to a dipole and a rectangular patch microstrip antenna to discuss about the complexities of the method.

In Chapter III the significance of current distribution and the experimental determination of the current distribution on a vivaldi antenna are discussed. Also the insertion loss characteristics of the antenna are given.

In Chapter IV an attempt is made to confine the antenna in an orthogonal coordinate system and better way of dividing the antenna into subdomains discussed. Approximate form of the subdomain functions are discussed.

In Chapter V summary and scope for further work in this area are discussed.

# CHAPTER II

## MOMENT METHOD

INTRODUCTION:

The vivaldi antenna consists of an exponential asymmetric slot line. [Fig. 2 ]. The antenna is etched on Cu clad Duroid sheet. The antenna radiation is in the end fire direction with the E-field in the x direction. The slot width of the radiating end and the length of the tapered slot line section are kept approximately same. When frequency is such that the slot width is approximately half wavelength, the radiator has high effeciency and can work effeciently beyond this frequency. The transition is made from a microstrip line to an assymetric slot line over a length of around half a wavelength and hence the input reflection coefficient increases as frequency is decreased below. The Fig. [ 2 ] also defines the coordinate axis for further analysis.

For a symmetric slot line [Fig. 3 ] the fields are given by

$$H_x = A\, H_o^{(1)} (K_c r)$$

$$H_r = \frac{A}{(1 - \lambda^*/\lambda)^2}\, H_1^{(1)} (K_c r)$$

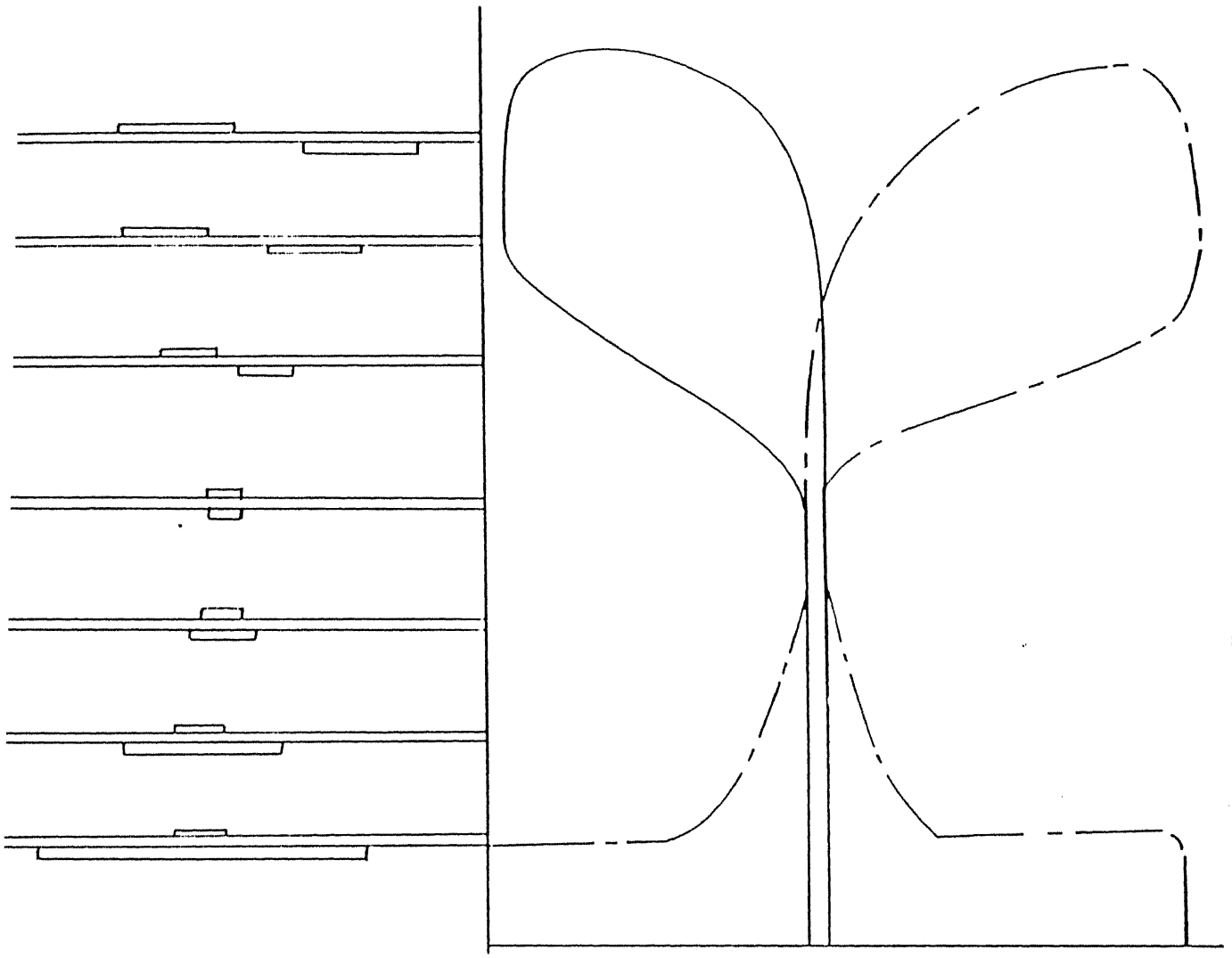

Fig. 2 Geometry of the fabricated vivaldi antenna

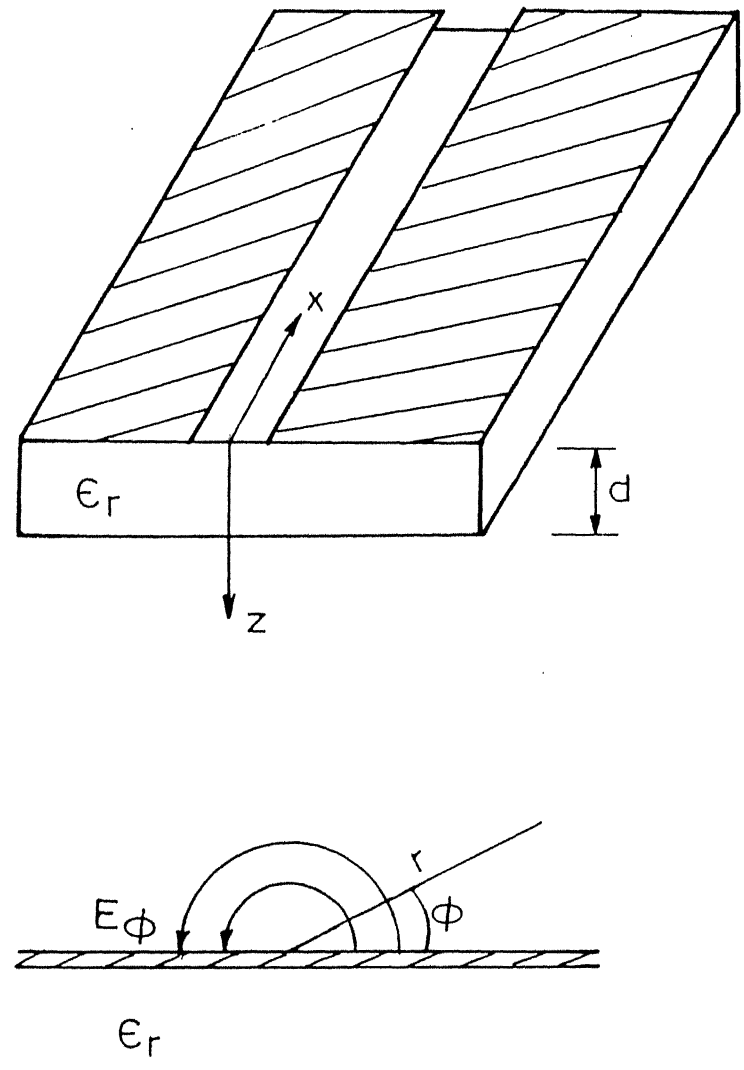


Fig.3 Geometry of a uniform slot line

$$E_{\phi} = -\eta \frac{\lambda^{*}}{\lambda} H_{r}$$

where $$K_{c} = j \frac{2\pi}{\lambda} \sqrt{\left(\frac{\lambda}{\lambda^{*}}\right)^{2} - 1}$$

$$\lambda^{*} = \lambda \sqrt{\frac{2}{\epsilon_{r}+1}}$$ is the wavelength in the dielectric

and $\eta$ = Intrinsic Impedance of air.

For $|x|$ large $H_{1}^{(1)}(x)$ and $H_{o}^{(1)}(x)$ may be written as

$$H_{n}^{(1)}(j|x|) = \frac{e^{-|x|}}{\sqrt{|x|}}$$

when $|x| = K_{c}r$.

It can be seen from the above equations that the higher the dielectric constant, the better will the slot line confine the fields very near it and function as a good transmission line. Hence a low dielectric constant material has to be chosen to make the tapered slot line work effectively as an antenna. The value of the dielectric chosen is 2.2 and the thickness is 1/32".

The advantage of the assymetric slot line antenna when compared to the symmetric slot line antenna which is present only on one side of the dielectric is that the input transition is better beause of the low impedance of the assymetric slot line, which can be easily matched to a microstrip line.

Also the double sided slot antenna can be used more effectively while designing a circular array for an omnidirectional antenna.

The two major subjects of vivaldi antenna design are:

(a) The transition from the main transmission line (usually microstrip) to a slot line, for feeding the antenna; this should have a wide operating frequency range and low reflection coefficient.

(b) The dimensions and shape of the antenna, to obtain the required beamwidth, bandwidth, sidelobes and backlobes.

The microstrip, the double parallel strip and the slotlines are all of 50 Ω impedance. A vivaldi antenna is fabricated and is used as a termination to the transition.

In order to evaluate the radiation pattern and the near field, the exact current distribution is required. Also the Input Impedance as a function of frequency can be evaluated once the current distribution is known. In order to find the current distribution the boundary conditions are satisfied on the antenna surface and an Integral equation obtained, which is later solved by a numerical technique such as the moment method.

FORMULATION OF THE INTEGRAL EQUATION:

The key to the solution of any antenna or scattering problem is a knowledge of the physical or equivalent current density distribution on the volume or surface of the antenna or scatterer. Once these are known then the radiated or scattered fields can be found using the standard radiation integrals. A main objective then of any solution method is to be able to calculate accurately the current densities over the antenna. This can be accomplished by the Integral Equation (IE) method.

In general there are many forms of Integral equations. Two

of the most popular for time harmonic electromagnetics are the Electric field Integral equation (EFIE) and the magnetic field integral equation (MFIE). The EFIE enforces the boundary condition on the tangential component of the electric field, whereas the MFIE enforces the boundary condition on the tangential components of the magnetic field.

The EFIE is based on the boundary condition that the total tangential electric field on a perfectly conducting surface of an antenna or scatterer is zero. This can be expressed as:

$$E_t = E_t^i + E_t^s = 0 \quad \text{on } s$$

or $$E_t^s = -E_t^i \quad \text{on } S.$$

where S is the conducting surface of the antenna or scatterer.

$E_t$ = Total tangential electric field.

$E_t^i$ = Incident tangential electric field and

$E_t^s$ = Scattered tangential electric field.

The incident field that impinges on the surface S of the antenna or scatterer induces on it an electric current density $\bar{J}_s$ which inturn radiates the scattered field. If $\bar{J}_s$ is known, the scattered field every where that is due to $\bar{J}_s$ can be found using the relation

$$E^s(r) = -j\omega\bar{A} - j\frac{1}{\omega\mu\epsilon}\nabla(\nabla \cdot \bar{A})$$

$$= -\frac{j}{\omega\mu\epsilon}\left[\omega^2\mu\epsilon\bar{A} + \nabla(\nabla \cdot \bar{A})\right]$$

where

$$\bar{A}(r) = \frac{\mu}{4\pi}\iint \bar{J}_s(r')\frac{e^{-j\beta R}}{R}\,dS'$$

hence

$$E^s(r) = -\frac{\eta}{\beta}\left[\beta^2\iint \bar{J}_s(r')\,G(\bar{r}, \bar{r}')\,ds'\right.$$

$$+ \nabla \iint \bar{J}_s(r') \, G(\bar{r}, \bar{r}') \, ds' \Big)$$

where,

$$G(\bar{r}, \bar{r}') = \frac{e^{-j\beta R}}{4\pi R} = \frac{e^{-j\beta |\bar{r} - \bar{r}'|}}{4\pi |\bar{r} - \bar{r}'|}$$

$$R = |\bar{r} - \bar{r}'|$$

If the observations are restricted on the surface of the antenna ($r = r_s$) then the above equation becomes

$$\frac{\eta}{\beta} \Big[ \beta^2 \int_S \int \bar{J}_s(r') \, G(\bar{r}_s, \bar{r}') \, ds'$$

$$+ \nabla \iint \nabla \bar{J}_s(r') \, G(\bar{r}_s, \bar{r}') \, ds' \Big] = E_t^i \; (r = r_s)$$

Because the right side of the equation is expressed in terms of the known incident electric field it is referred to as the electric field integral equation (EFIE). It can be used to find the current density $\bar{J}_s(r')$ at any point $r = r'$ on the antenna or scatterer. Once the integral equation is obtained it is solved numerically by a method such as the moment method.

THE MOMENT METHOD:

There are various methods to obtain the exact current distribution, prominent among them being spectral domain technique, immittance approach, transmission line modelling, moment method etc. All of the above methods and many more can be used to obtain the solution of the integral equation which is the basic equation having the information about the current distribution.

Analytical solution of the integral equation is rarely possible to obtain, and in almost all the cases numerical

techniques are used, the most common being the moment method, [10] knowing the voltage at the feed terminals and determining the current distribution, the input impedance and the radiation pattern can then be obtained.

An integral equation is of the form

$$F(g) = h \qquad -(1)$$

where F is a known linear (integral) operator, h is a known excitation function and g is the resonse function. The objective here is to determine g once F and h are specified. Though the solution is often not possible in closed form, the linearity of the operator F makes a numerical solution possible. The technique known as the moment method requires that the unknown response function is expanded as a linear combination of N terms and is written as

$$g(z') \cong C_1 g_1 (z') + C_2 g_2 (z') + \ldots C_N g_N (z') = \sum_{n=1}^{N} C_n g_n (z')$$

Each $C_n$ is an unknown constant and each $g_n (z')$ is a known function referred to as basis or expansion function. Equation (1) reduces to

$$\sum_{n=1}^{N} C_n F(g_n) = h \qquad -(2)$$

The basis functions $g_n$ are chosen so that each $F(g_n)$ can be evaluated conveniently, preferably in closed form or at the very least numerically. The only task then is to find the $C_n$; the N unknown constants.

**BASIS FUNCTIONS:**

One very important step in any numerical solution is the

choice of basis functions. In general one choses as basis functions, the set which has the ability to accurately represent and resemble the anticipated unknown function, while minimising the computational effort required to employ it. These basis functions are divided into two general classes the subdomain function, which are non zero only over a part of the antenna surface and the continuous entire domain functions which are non zero over the entire antenna. Some examples of the subdomain functions being piecewise constant, piecewise linear, piecewise sinusoid etc. as in Fig.4 . A common entire domain basis set is that of a sinusoidal function. The main advantage of entire domain bases lies in problems where the unknown function is assumed apriori to follow a known pattern. In such cases, entire domain functions may render an acceptable representation of the unknown while using far fewer terms in the expansion than would be necessary for subdomain bases.

Eqn. (2) is a linear equation with N unknowns and hence to obtain the N unknowns we define the inner product

$$< w, g > = \int\int_S w.g \, ds$$

where S is the surface of the structure being analysed and w is the weighting function. The equation then reduces to a matrix equation

$$\left[ F_{mn} \right] \left[ C_n \right] = \left[ h_m \right]$$

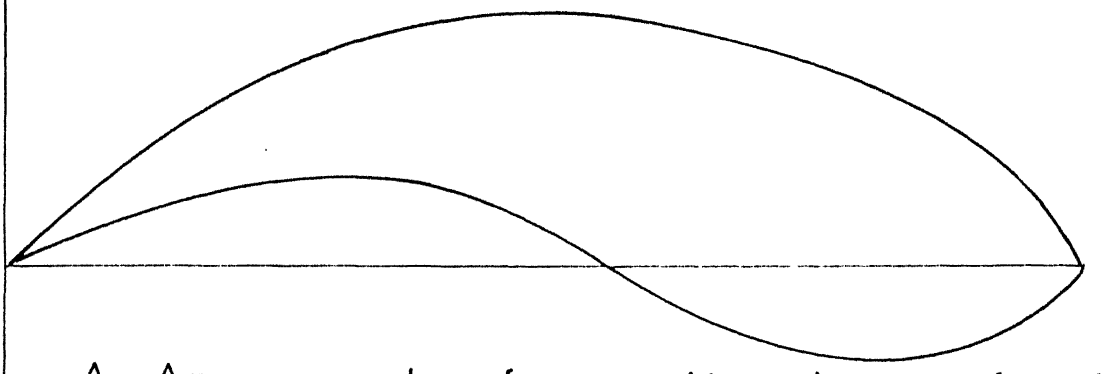

A. An example of an entire domain function

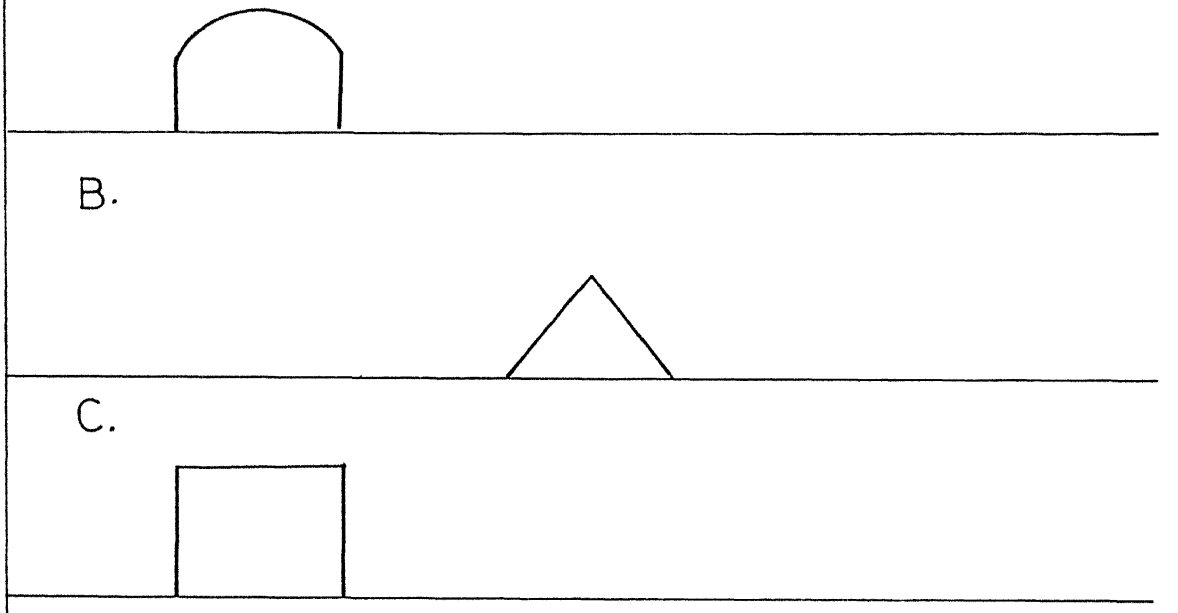

B.

C.

D. Some subdomain functions

Fig 4

where

$$\left[ F_{mn} \right] = \begin{bmatrix} \langle w_1, F(g_1) \rangle & \langle w_1, F(g_2) \rangle & \cdots \\ \langle w_2, F(g_1) \rangle & \langle w_2, F(g_2) \rangle & \cdots \\ \vdots & \vdots & \vdots \end{bmatrix}$$

$$\left[ C_n \right] = \begin{bmatrix} C_1 \\ C_2 \\ \vdots \\ C_n \end{bmatrix} \qquad \left[ h_m \right] = \begin{bmatrix} \langle w_1, h \rangle \\ \langle w_2, h \rangle \\ \vdots \\ \langle w_n, h \rangle \end{bmatrix}$$

The matrix equation may be solved by inversion and can be written as

$$\left[ C_n \right] = \left[ F_{mn} \right]^{-1} \left[ h_m \right]$$

As special cases if weighting functions are chosen to be same as basis functions, then it is called Galerkin's method and if they are chosen as delta functions then it is called point matching.

MOMENT METHOD APPLIED TO A DIPOLE:

To illustrate the solution outlined above we display the results for a dipole of length 0.5 $\lambda$ and diameter = 0.005 $\lambda$. The subdomain bases functions used are pulse functions and weighting functions used are delta functions. We would have assumed the current distribution on a dipole to be sinusoidal, but though the

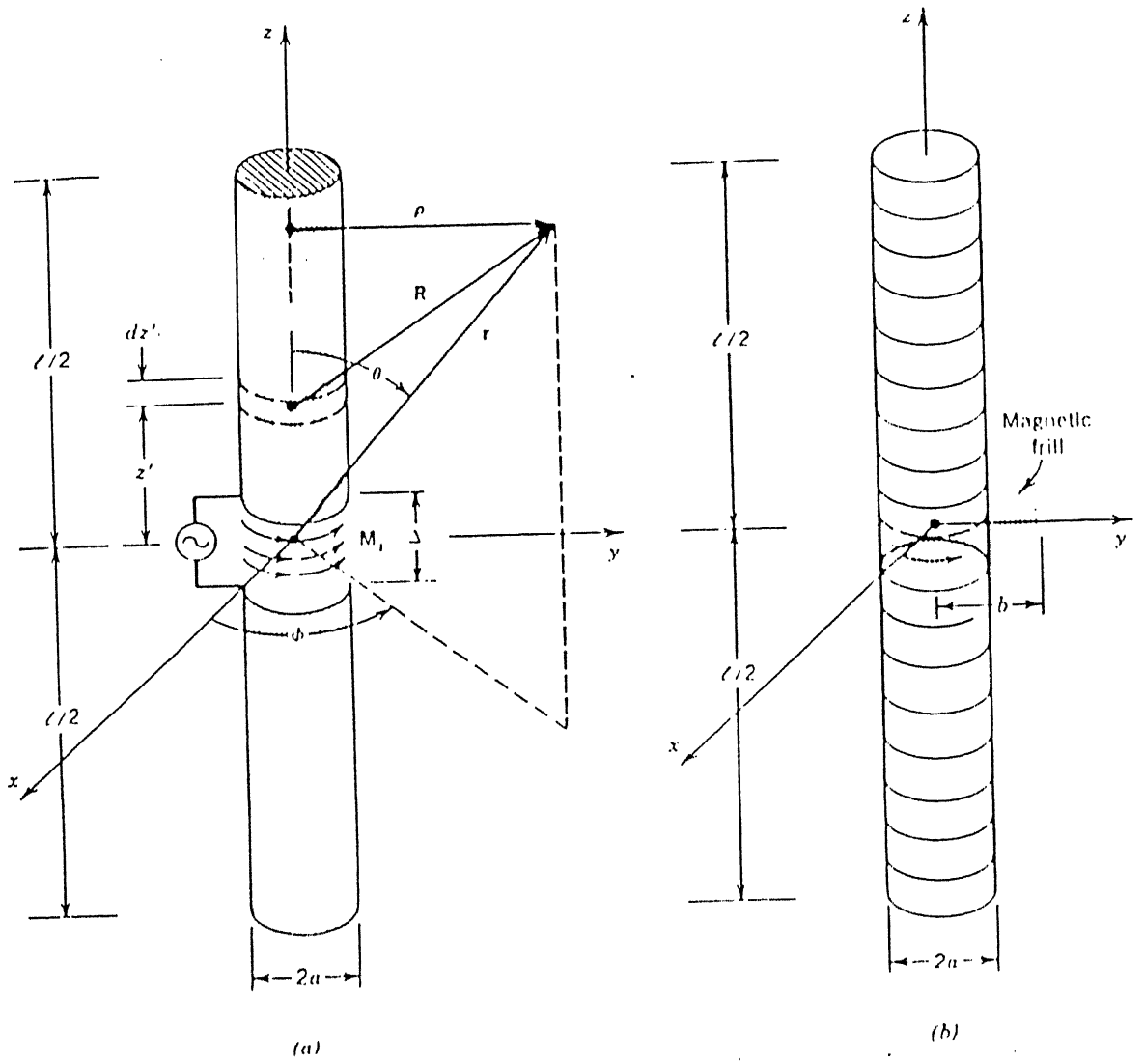


Fig. 5 Dipole with the two different source models

| N | DELTA GAP | MAGNETIC FRILL |
|---|---|---|
| 7 | 122.8 + j 113.9 | 26.8 + j 24.9 |
| 11 | 94.2 + j 49.0 | 32.0 + j 16.7 |
| 21 | 77.7 − j 0.8 | 47.1 − j 0.2 |
| 29 | 75.4 − j 6.6 | 57.4 − j 4.5 |
| 41 | 75.9 − j 2.4 | 68.0 − j 1.0 |
| 51 | 77.2 + j 2.4 | 73.1 + j 4.0 |
| 61 | 78.6 + j 6.1 | 76.2 + j 8.5 |
| 71 | 79.9 + j 7.9 | 77.9 + j 11.2 |
| 79 | 80.4 + j 8.8 | 78.8 + j 12.9 |

TABLE Input impedance caluculated with different values of N

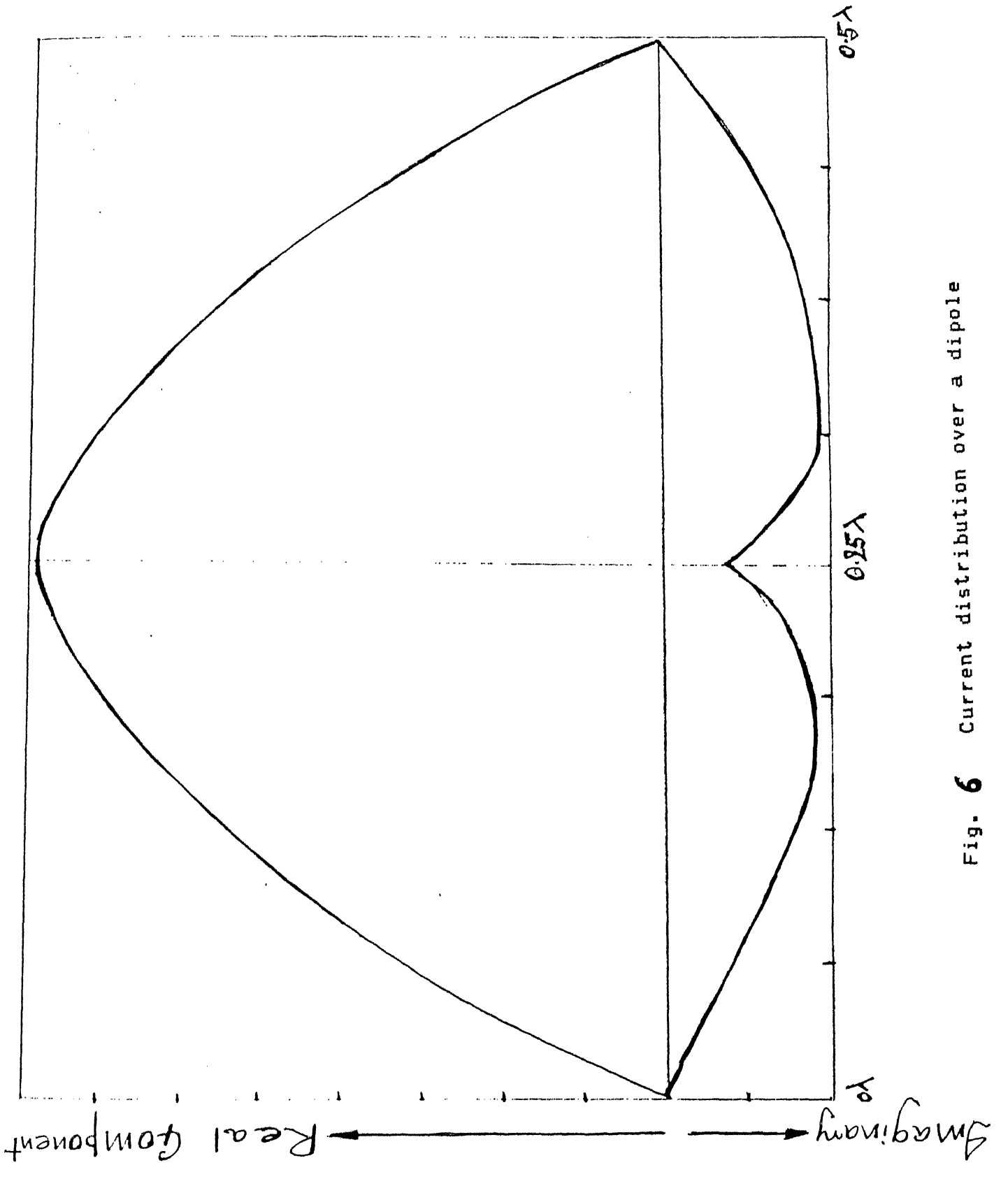


Fig. 6 Current distribution over a dipole

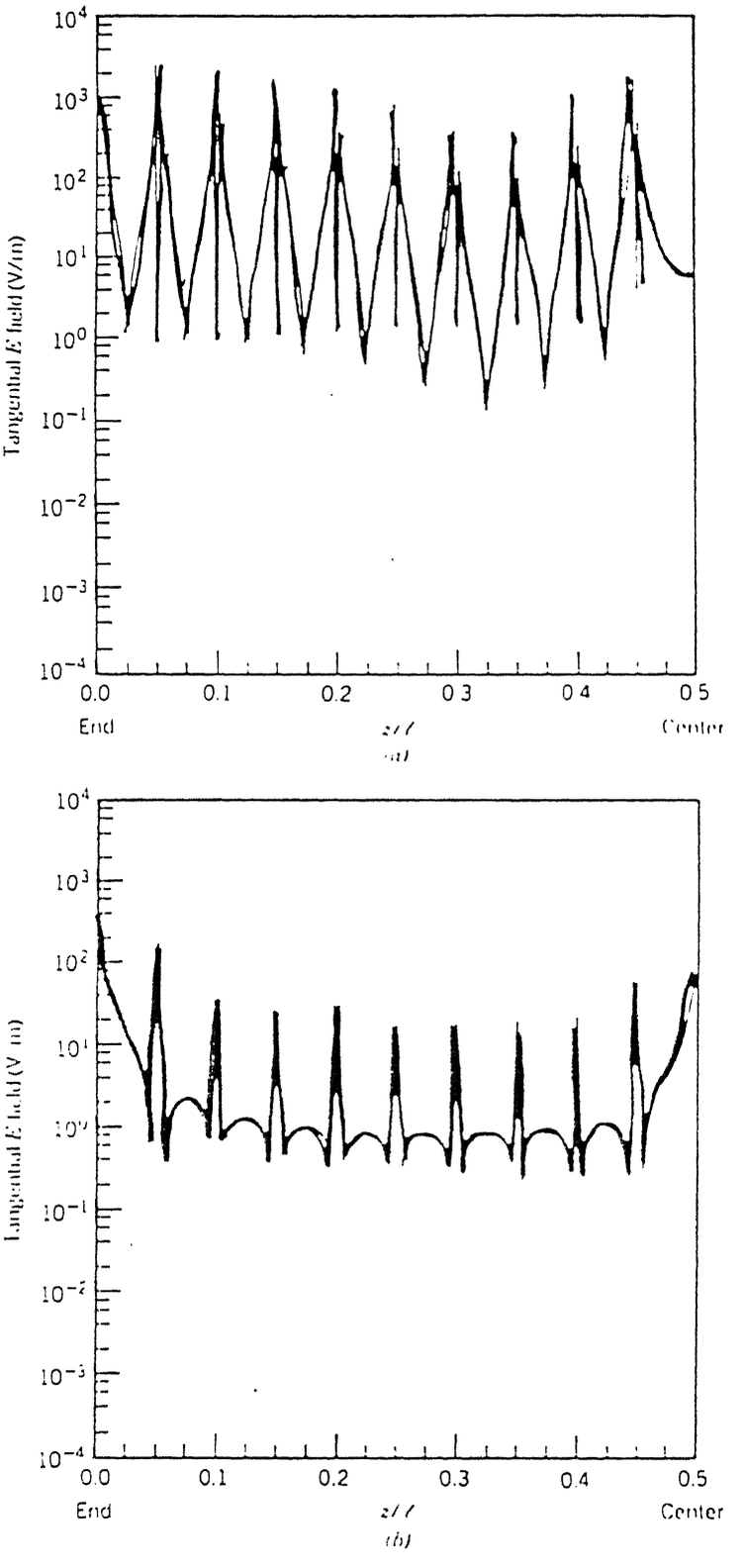


Fig. 7 Residuals as calculated using

(a) pulse bases and point matching

(b) Galerkins method [10]

magnitude of the current does have a sinusoidal form, the standing wave pattern is not completely valid, in the sense that there are phase variations in the current along the antenna length. Thus the information about the reactive portion of the current is obtained by applying moment method.

The current distribution and the Input Impedance calculated for a dipole in Fig.[5] is shown in the Fig.[6] and Table

From the Fig. [6] it is clear that the current distribution on a dipole is having a real and an imaginary part. The real part is greater in magnitude than the imaginary part and is more or less sinusoidal. The real part is the major contributor for the far field pattern and this is the reason for obtaining a good idea about the radiation pattern of the dipole even if we assume a sinusoidal current distribution with a constant phase. Though the actual current is not truly sinusoidal with the same phase. The sinusoidal distribution with same phase completely fails to give zero electric field on the dipole surface because, the imaginary part has a considerable contribution towards the near field. When the actual current distribution is used then the tangential electric field is found to be negligible on the whole of the antenna when compared to the field at the excitation point. It is found to have the following form:

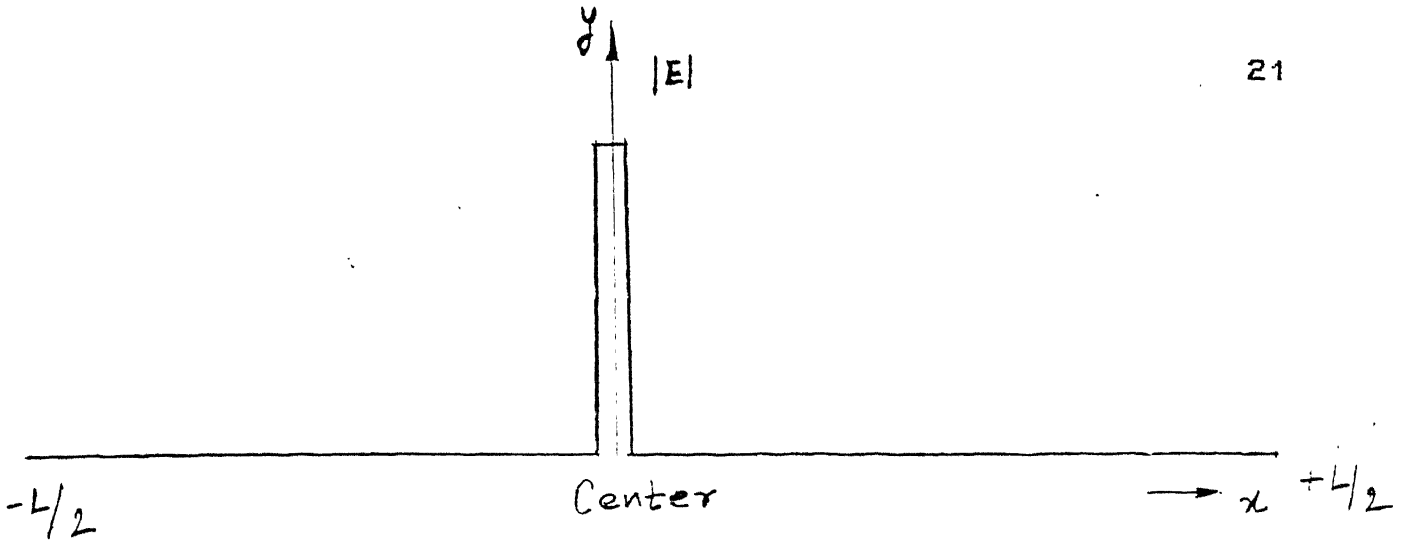


The values of the input impedance are calculated for two different type of source modelling: (a) the deltagap modelling and (b) the magnetic frill modelling.

For finding the radiation pattern accurately the source modelling might not play an important role because one deals with far field which is not a very sensitive function of current distribution, but for the calculation of the input impedance, source modelling is a significant factor. The way we model the source should be an accurate representation of the actual source. For the case of the cylindrical dipole a coaxial fed monopole would be better represented at its excitation point by a magnetic frill whereas a delta gap would be a better representation for a twin wire feed.

Also since point-matching is a method whose solutions satisfy the electromagnetic boundary conditions (vanishing tangential electric fields on the surface of an electric conductor) only at discrete points, the boundary conditions may not be satisfied at the in between points and the deviation is known as the residual [10]. For a half wavelength dipole, a typical residual is as shown in Fig.[7]. The residual decreases

if Galerkins method instead of point matching is used. The results for Galerkins method are shown in Fig.[7].

MOMENT METHOD AS APPLIED TO MICROSTRIP ANTENNAS:

A microstrip antenna consists of a metallic plate or patch on a dielectric slab [Fig.8]. The patch is fed either by a microstrip transmission line contacting an edge of patch or by a coaxial probe extending through the ground plane and contacting the patch.

The microstrip patch when fed by a microstrip line and a coaxial proble will have different source models. In the former case the microstrip feed line can be replaced by an equivalent current source which is obtainable from the transverse electric or magnetic fields ($\bar{E}_t$ or $\bar{H}_t$) in the plane where the microstrip feed line connects to the patch as shown in Fig. [9]. The transverse fields can be represented by the TEM feed line fields

$$\bar{E}_t = -\hat{z}\frac{V_o}{\sqrt{w_1 z'}} \quad \text{and} \quad \bar{H}_t = -\hat{y}\frac{I_o}{\sqrt{w_1 z'}}$$

where $w_1$ is the effective width $w_1 = w + \Delta w$ where w is the strip width and $\Delta w$ is an extension which accounts for the fringing fields at the edges of the feed line. From uniqueness concepts $\bar{H}_t$ backed by a perfect magnetic conductor is needed; therefore the microstrip feed line can be replaced by an electric current source $\bar{J}_s = I_o \hat{\psi}$ where $\hat{\psi} = \hat{z} / \sqrt{w_1 z'}$ . Likewise for a probe fed patch, the probe can be replaced by an equivalent current source

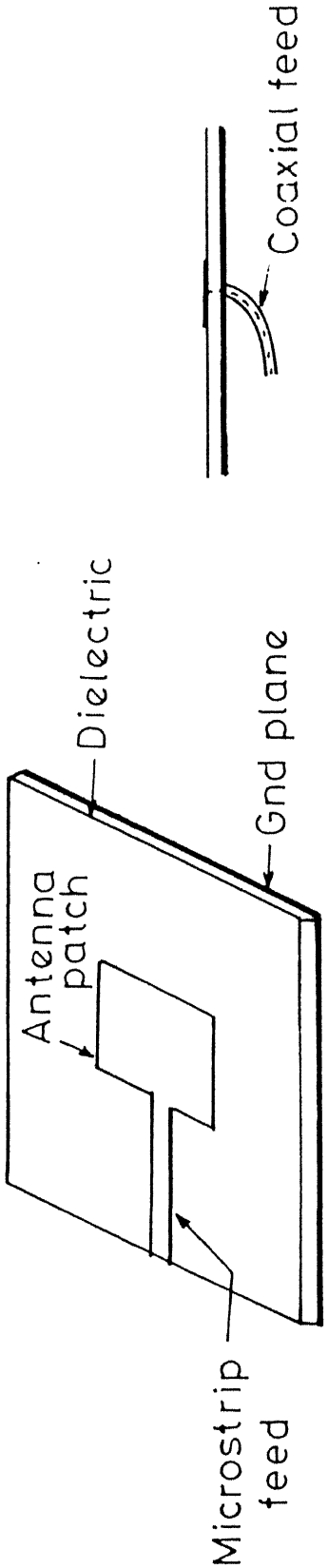


Fig. 8 Geometry of a microstrip patch antenna

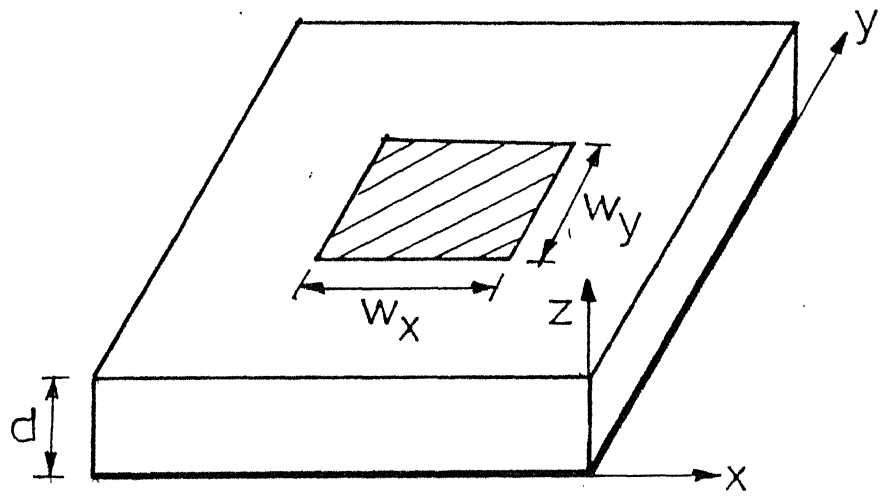


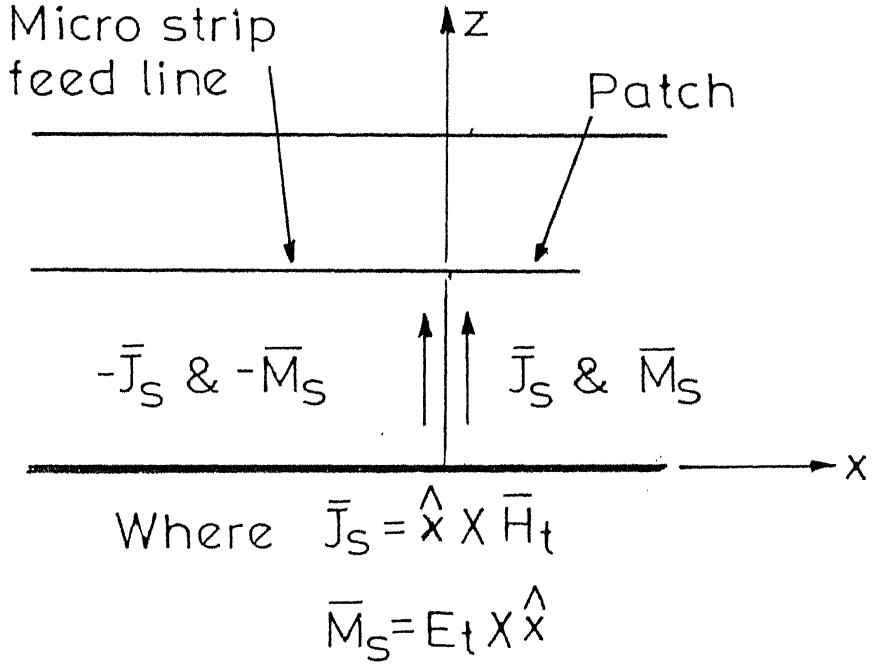


FIG·9 GEOMETRY OF A MICROSTRIP ANTENNA AND EQUIVALENT OF A MICROSTRIP ANTENNA EXCITED BY A MICROSTRIP FEED LINE

$\bar{J}_s = I_o \hat{\psi}$ present on a cylindrical surface with diameter equal to $d_o$ where $\hat{\psi} = \hat{z} / (\pi d_o)$ and $d_o$ is the diameter of the probe.

Moment method can be used to solve the microstrip antenna [11]. The method is based upon a boundary condition or integral equation formulation, with the unknowns being the currents on microstrip patches and the wire feed lines plus their images in the ground plane. The integral equation is solved using the method of moments. The integral equation is formulated with the zero reaction concept [12] developed by Rumsey.

THE REACTION TECHNIQUE:

Consider the exterior scattering problem illustrated in the Fig.[10]. In the presence of a dielectric or conducting body, the impressed electric and magnetic currents ($\bar{J}_i$, $\bar{M}_i$) generate the electric and magnetic field intensities ($\bar{E}$, $\bar{H}$). Let the exterior medium be free space.

From the surface equivalence theorem of Schelkunoff [10], the interior field will vanish (without disturbing the enterior field) if we introduce the following surface current densities

$$\bar{J}_s = \hat{n} \times \bar{H}$$

$$\bar{M}_s = \bar{E} \times \hat{n}$$

on the closed surface S of the scatterer. In this situation, illustrated in Fig.[10] we may replace the scatterer with free space without disturbing the field anywhere.

By definition, the incident field ( $\bar{E}_i$, $\bar{H}_i$ ) is generated by ( $\bar{J}_i$, $\bar{M}_i$ ) in free space, and the scattered field is

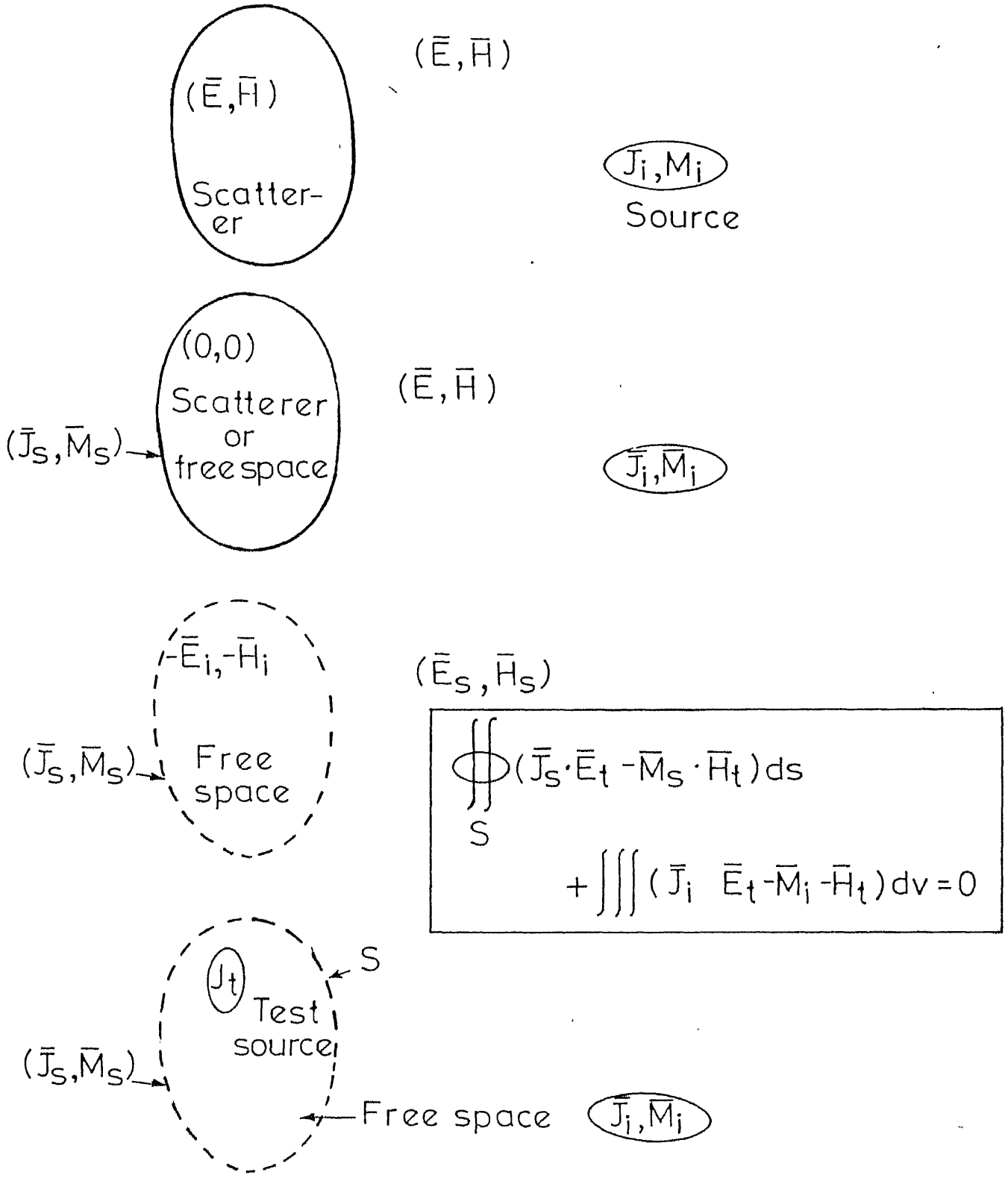


FIG.10 ZERO REACTION THEOREM

$$\bar{E}_s = \bar{E} - \bar{E}_i$$

$$\bar{H}_s = \bar{H} - \bar{H}_i$$

when the surface current ( $\bar{J}_s$, $\bar{M}_s$ ) radiates in free space, it generates the field ( $\bar{E}_s$, $\bar{H}_s$ ) in the exterior and ($-\bar{E}_i$, $\bar{H}_i$ ) in the interior region. The result is shown in Fig. [10] . We place an electric test source $\bar{J}_t$ in this region and find from the reciprocity theorem that

$$\iint ( \bar{J}_s \bar{E}_t - \bar{M}_s \bar{H}_t ) dS + \iiint ( \bar{J}_i \bar{E}_t - \bar{M}_i \bar{H}_t ) dv = 0$$

where ($\bar{E}_t$, $\bar{H}_t$) is the free space field of the test source. The above equation is the integral equation for the scattering problem and this can be converted into a matrix equation using moment method. We get

$$[Z]\,[I] = [V]$$

Typical terms of z and V are as given below:

$$Z_{mn} = -\int_n \bar{E}^m \cdot \bar{J}_n \, ds$$

$$V_m = \int_n \bar{E}^m \cdot \bar{J}_i \, dl$$

where the surface current $\bar{J}_s$ has been expanded as

$$\bar{J}_s = \sum_{n=1}^{N} I_n \bar{J}_n \text{ and}$$

$\bar{J}_i$ is the impressed current filament.

MODIFICATION FOR DIELECTRIC SLAB:

If there is a dielectric slab present in the antenna then the slab is removed and replaced by free space and the equivalent volume polarization currents

$$J_v = jw (\epsilon - \epsilon_o) E$$

The matrix equation then gets modified to

$$[ Z + \Delta Z ] [I] = [V]$$

where

$$\Delta Z_{mn} = - jw (\epsilon - \epsilon_o) \int_V \bar{E}^m . \bar{E}^n_d \, dv$$

where $\bar{E}^n_d$ is the electric field radiated by $\bar{J}_n$ the n-th expansion mode in the presence of the dielectric slab, and $\bar{E}^m$ is still the free space field of the m-th test mode. For a microstrip antenna with ground plane $\bar{E}^n_d$ is given in a simplified manner in [13]. For our problem use of Sommerfeld integrals is required for the evaluation of $\bar{E}^n_d$. The feed model is a very important factor determining the accuracy of the results obtained.

Once current distribution is known then the input impedance and radiation pattern can be easily found.

RECTANGULAR PATCH MICROSTRIP ANTENNA:

To illustrate the method outlined above a rectangular patch antenna without dielectric has been analysed and the results presented. The geometry of the antenna is shown in Fig.[11] along with the results. There are serious limitations if rectangular pulse bases are used and the maximum cell width is restricted to 0.1 $\lambda$ when the size of the antenna is greater than 2 or more square wavelengths in area.

Here use is made of sinusoidal reaction formulation as given by Richmond [14]. In this method the surface of the antenna is divided into cells and the surface current distribution is expanded in overlapping sinusoidal bases in the direction of

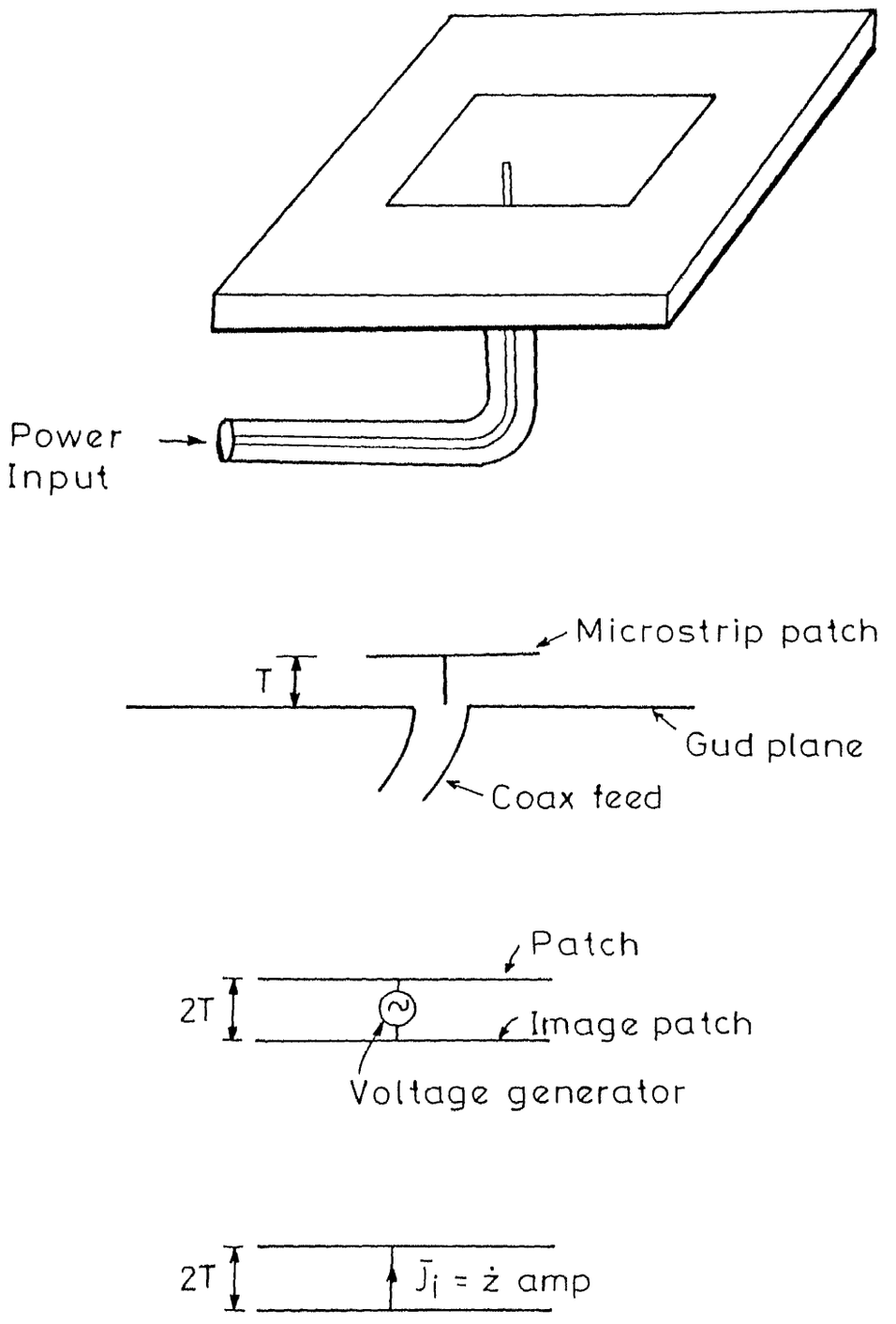


Fig.11 Coaxially fed microstrip patch antenna

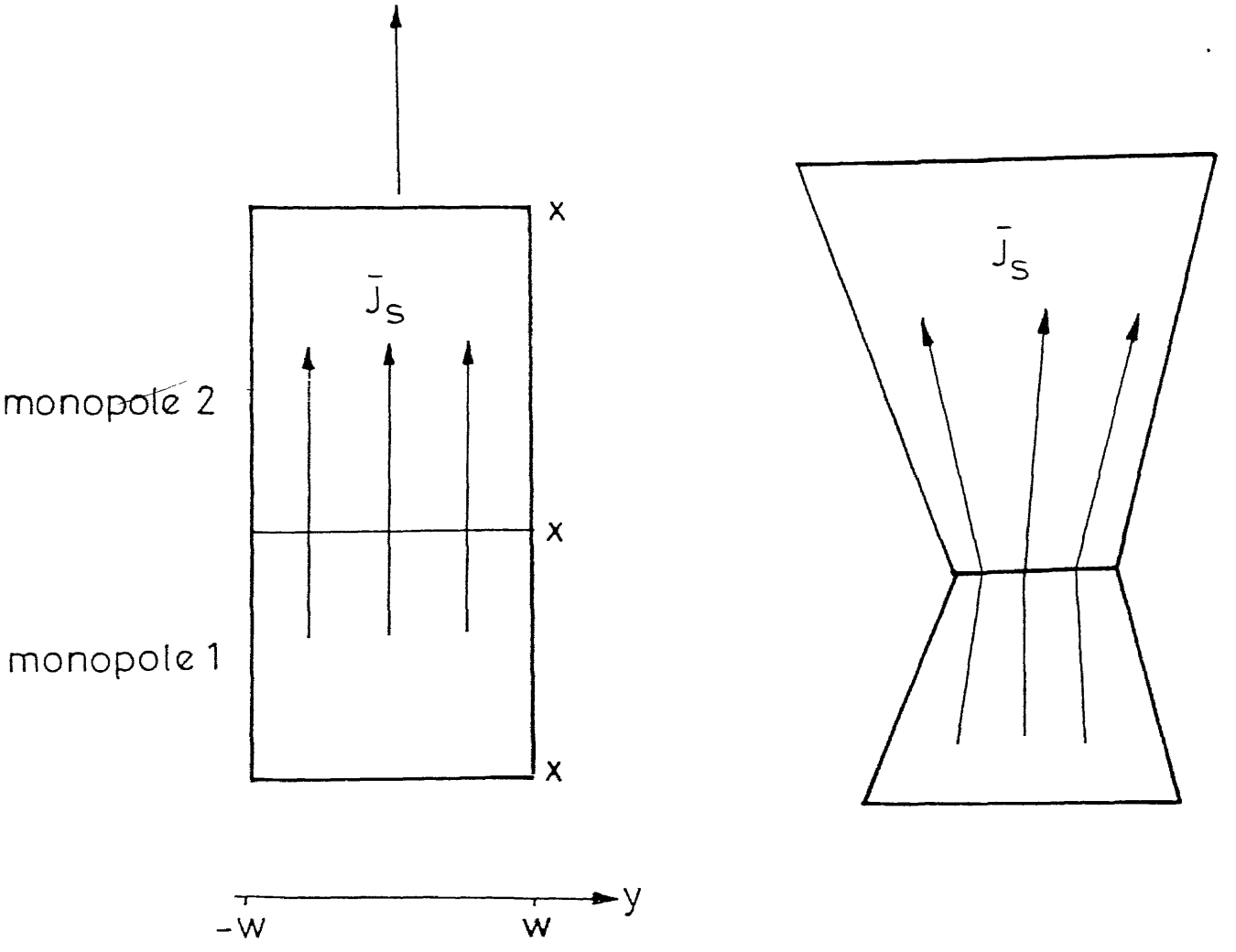


Fig.12 Rectangular and quadrilateral surface patch dipoles

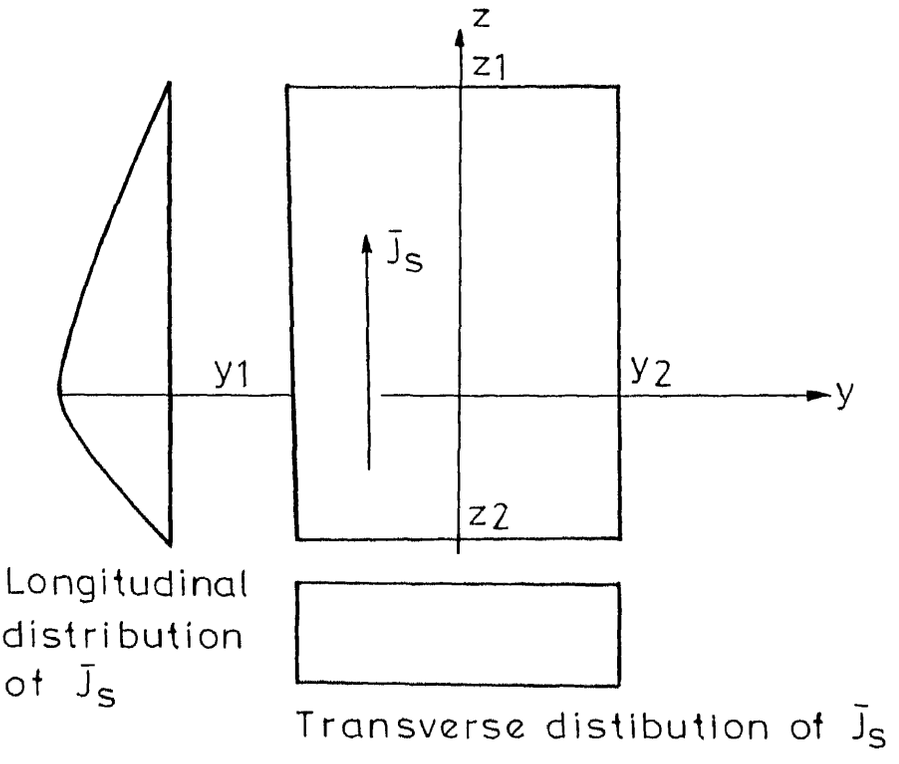


$$\bar{J}_s = \frac{\hat{z}\,\gamma\left[I_1 \sinh\gamma(z_2-z) + I_2 \sinh\gamma(z-z_1)\right]}{2\sinh(\gamma h)\sinh(\gamma w)}$$

Fig.13 Sinusoidal surface patch dipole

current flow and rectangular pulse bases in the transverse direction as in Fig. [12] via an application of Galerkins method, the integral equation formulated with the zero reaction concept is reduced to a matrix equation.

$$\begin{bmatrix} Z_{bb} & Z_{bt} \\ Z_{tb} & Z_{tt} \end{bmatrix} \begin{bmatrix} I_b \\ I_t \end{bmatrix} = \begin{bmatrix} V_b \\ V_t \end{bmatrix}$$

where the subscript b refers to the bottom plate and t refers to the top plate. From symmetry of the problem we have

$I_t = -I_b$ and $Z_{tt} = Z_{bb}$, $Z_{tb} = Z_{bt}$ and

$V_t = -V_b$ as a consequence of which

$$I_t = I_b = \frac{V_t}{Z_{tt} - Z_{tb}} .$$

The results for an antenna which is 15 cms by 7.5 cms is given in the Fig. [13].

Also the basis function of sinusoidal form [Fig 14] over a patch has the advantage that it has the exact expressions for the near field and hence resulting in reduction of one order of numerical integration [14] in calculating the impedance elements of the impedance matrix. In general the sinusoidal basis functions closely approximate many wave forms and also helps in reducing the number of elements or order of impedance matrix because of their greater domain.

The rectangular microstrip antenna with a ground plane is found to be resonant at a frequency of 933 MHz and a small bandwidth.

Element in free space Impedance matrix

| Frequency(MHz) | Ztt | Ztb |
|---|---|---|
| 932.0 | 60.5368 + j 4.9816 | 60.4877 + j 4.9874 |
| 932.2 | 60.5748 + j 5.0154 | 60.5257 + j 5.0199 |
| 932.4 | 60.6128 + j 5.0491 | 60.5636 + j 5.0523 |
| 932.6 | 60.6508 + j 5.0828 | 60.6016 + j 5.0848 |
| 932.8 | 60.6889 + j 5.1165 | 60.6396 + j 5.1173 |
| 933.0 | 60.7270 + j 5.1503 | 60.6777 + j 5.1498 |
| 933.2 | 60.7651 + j 5.1840 | 60.7158 + j 5.1823 |
| 933.4 | 60.8033 + j 5.2177 | 60.7538 + j 5.2147 |
| 933.6 | 60.8415 + j 5.2514 | 60.7920 + j 5.2472 |
| 933.8 | 60.8796 + j 5.2851 | 60.8301 + j 5.2797 |

Observations

Ztt = self impedance = Rs + j Xs

ztb = mutual impedance = Rm + j Xm

1) Always Rs > RM
but Rs Rm

2) Xs > Xm if frequency > 933.0 MHz

Xs < Xm if frequency < 933.0 MHz

Xs = Xm somewhere near frequency = 933.0 MHz

The dipole and the microstrip patch were easily solved because of the fact that they were simple in structure and confined to a coordinate system. The solutions can be more accurately and quickly obtained if the approximate current distribhution which is known a priori is used as entire domain functions. In the case of rectangular patch microstrip antenna use was made of sinusoidal surface patch dipoles which are entire domain functions for this problem.

# CHAPTER III

## MEASUREMENT OF CURRENT DISTRIBUTION ON VIVALDI ANTENNA

### INTRODUCTION:

Hidden in the integral equation is the information about the current and once it is known, it can be used to find the radiated fields using the equation

$$\bar{E}^{s}(r) = -j w \bar{A} - j \frac{1}{w \mu \epsilon} \nabla (\nabla . \bar{A})$$

where $\bar{A}$ is the vector potential.

The most important properties of an antenna, the radiation pattern and the input impedance are dependant solely on the current distribution. Though there can be an intuitive feel of the form of current distribution (like assuming a sinusoidal distribution over a dipole), the exact value of the current at each point is required to obtain the radiation pattern and the input impedance. Though an approximate form may give a fairly good picture of the radiation pattern, it completely fails to give a correct value for the input impedance and the near field [7]. The knowledge of the exact current distribution is felt all the more necessary when one has to deal with antenna arrays where antennas are placed very near to each other and the near field of the neighbouring antennas is felt on them. Analytical solutions

of the integral equation are possible rarely and can be found only for two or three cases of antennas like spheroidal antennas where the antenna confines itself to a particular coordinate system. If the antenna is of any other shape there is no other way than to resort to approximations and numerical techniques like moment method to solve for the current distribution.

The moment method formulation requires the appropriate selection of the basis functions and weighing functions. A wrong selection of the basis functions and weighing functions may not give accurate results unless the number of iterations are many which in turn means a lot of computer time. The weighing functions play an important role in the sense that they are the ones which decide the forcing of the boundary conditions. Using weighing functions like delta functions might lead to very poor results because the boundary conditions are satisfied at only very few discrete points, whereas galerkins method of choosing the same basis functions as weighing functions gives better results because of the fact that the boundary conditions are satisfied on an average over the surface of the antenna and not at discrete points. Also the number of terms required will be very less for convergence if the entire domain functions are used and better results will be obtained if they closely approximate the actual current distribution. For some antennas like dipole it is easy to choose the entire domain functions as sinusoidal functions because it closely approximates the actual current distribution on the antenna.

Hence an attempt is made to get an approximate form of current distribution on the antenna by measurement.

EXPERIMENTAL MEASUREMENT OF CURRENT DISTRIBUTION:

Since it has been observed that the current distribution is the most important fator which determines the radiation pattern and input impedance, we will explain methods to find the current distribution experimentally. Measurement of the current on the surface of an antenna involves measurement of the tangential magnetic field very near this surface. These measurements are made in the reactive near field of the antenna, and the requirement that they be made in very close proximity to the antenna may dictate the use of very small probe antennas to sample these fields. From an experimental point of view, the problem is to design or obtain probes or receiving antennas with associated apparatus for determining the amplitude, phase and polarization of the electromagnetic field at any point in space, in the immediate vicinity, including the surface, of radiating antenna.

SAMPLING PROBE - THEORY AND DESIGN:

On a perfectly conducting surface, the surface current density $\overline{J}$ is related to the magnetic field by the relation

$$\hat{n} \times \overline{H} = \overline{J}$$

where $\hat{n}$ is the unit normal directed outward from the surface. The depth of penetration of the tangential magnetic field in a good conductor is so small in and above the VHF range of

frequencies that the true current distribution is very closely approximated by the surface distribution on a perfect conductor. Thus if the output of a probe is proportional only to the magnitude of the magnetic field it may be considered to be a measurement of the true surface current. Suitable probe for the measurement of the tangential magnetic field is an infinitesimal magnetic dipole which to a good approximation may be realised by a small loop antenna.

The following requirements are to be met by the probe if an accurate measure of the current is required [8].

1. Probe should not distort the field.
2. Probe should be so small as to represent a point.
3. Probe should have the desired polarization
4. The output should be of a magnitude, capable of being measured.

Simple loop – The loop antenna consists of a single turn of wire as shown in Fig. [15].

If the loop is small and the magnetic field uniform then the current $I_H$ induced in the loop by the magnetic field is equal in magnitude at all points on the contour. The total current through the load is

$$I_L = I_H + I_z + I_y$$

where $I_H$ is due to the magnetic field and $I_z$, $I_y$ are due to the electric field. Due to symmetry $I_z$ does not contribute to the current but $I_y$ if present contributes to the load current. Hence it is required to keep the loop in such a way that $\bar{E}$ field is

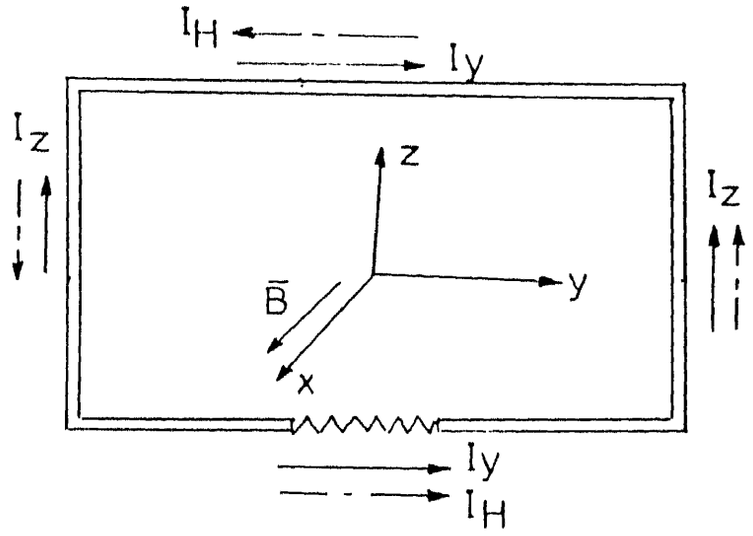


A. Circuit equivalent of a singly loaded loop

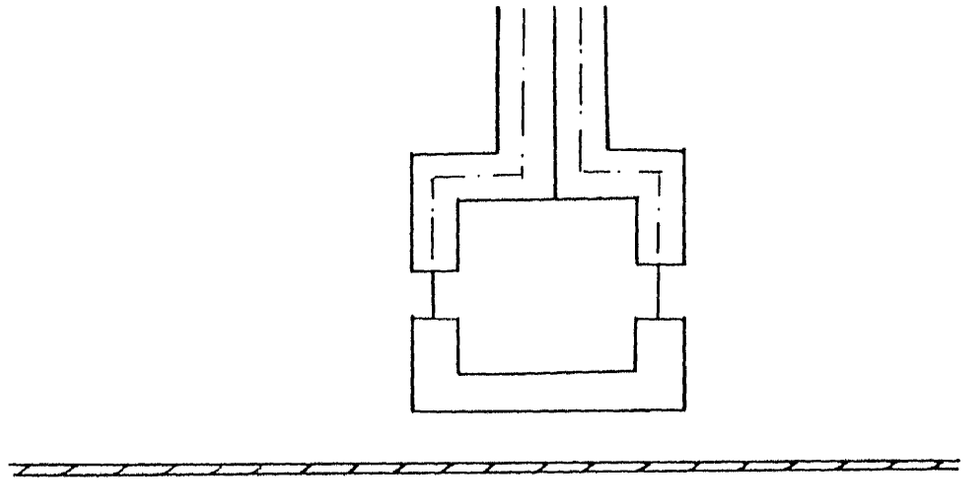

B. A doubly loaded sampling probe

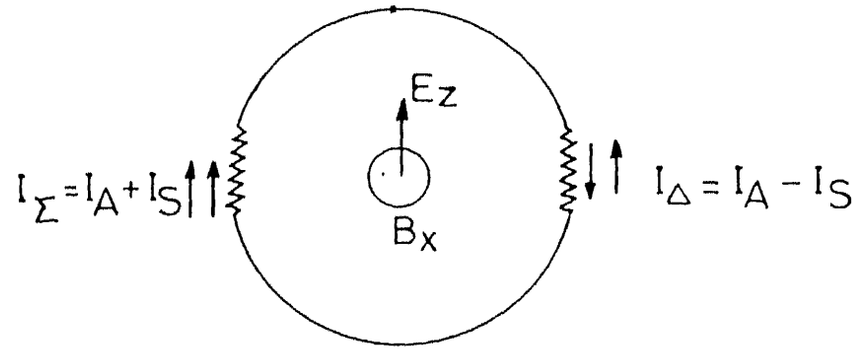


Fig 15 C. Circuit equivalent of a doubly loaded loop

tangential to the symmetric portion of the loop.

The magnetic sensitivity of small loops is proportional to the loop area and hence the loop must be of sufficient size to provide a useful output. Balanced against this is the fact that the output of the probe is proportional to the average value of the magnetic field through the loop aperture, hence the aperture must be small enough to essentially measure the field at a point. (Also the presence of non-vanishing longitudinal electric field at points away from the antenna surface means that the magnetic field away from the surface is no longer exactly proportional to the current).

To overcome the above mentioned difficulty double loaded loops [Fig.16] are used.

The total current in $Z_L$ due to the fields across the two gaps can be resolved into symmetric and antisymmetric components. The symmetric components $I_s$ are proportional to $B_x$ and antisymmetric components $I_A$ are proportional to $E_z$.

In a practical system $I_B$ and $I_E$ can be obtained by using a $180^0$ hybrid.

$$I_B = I_I + \nu I_\Delta$$
$$I_E = I_\Delta + \nu I_I$$

where $\nu$ is the isolation of the hybrid.

DESIGN OF A-D CARD:

The measurement of the tangential magnetic field involves movement of the probe all over the antenna in a predetermined fashion and then noting down the values of the position of the

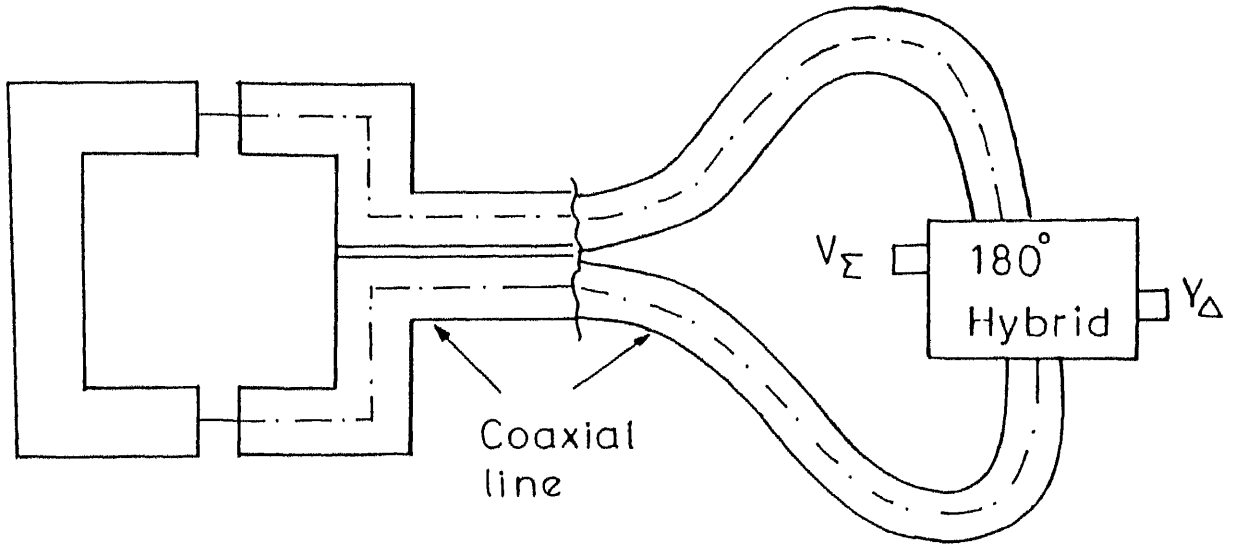


Fig. 16 Doubly loaded sampling probe

probe, values of amplitude and phase of the received power $S_{21}$. But this recording involves a lot of strain and inaccuracy in measurement due to the large number of values to be recorded. Also the noted values have to be later entered on to a P.C. to get an idea of the approximate form of current distribution.

The above difficulty has been overcome by designing a PC card which with the associated software helps us to record the values directly on to the P.C. The total set-up is shown in Fig. ( 17 ). The input to the PC Card is from the rear panel of the network analyser which gives a voltage of 10 mv/dB for amplitude and 50 mv/degree for phase. Thus by properly calibrating the A-D converter we can directly get the values of amplitude and phase on to the PC which can be stored in a file and later graphs of it can be viewed.

The block diagram of the PC Card is shown in the Fig. [18 ]. It can be extended to include more channels so as to get a direct measure of frequency also.

DESIGN DETAILS:

An extension of PC's 8088 $\mu$p-bus called I/o channel is available on eight, 62 pin edge connectors [9] [Fig. 19 ]. Any non system hardware, with proper decoding scheme can be put on this bus and accessed by the CPU.

The I/o channel contains an 8 bit bidirectional data bus, 20 address lines, 6 levels of interrupt, control lines for memory and I/o read or write, clock and timing signals, a channel check line, 3 channels of DMA control lines, memory refresh timing

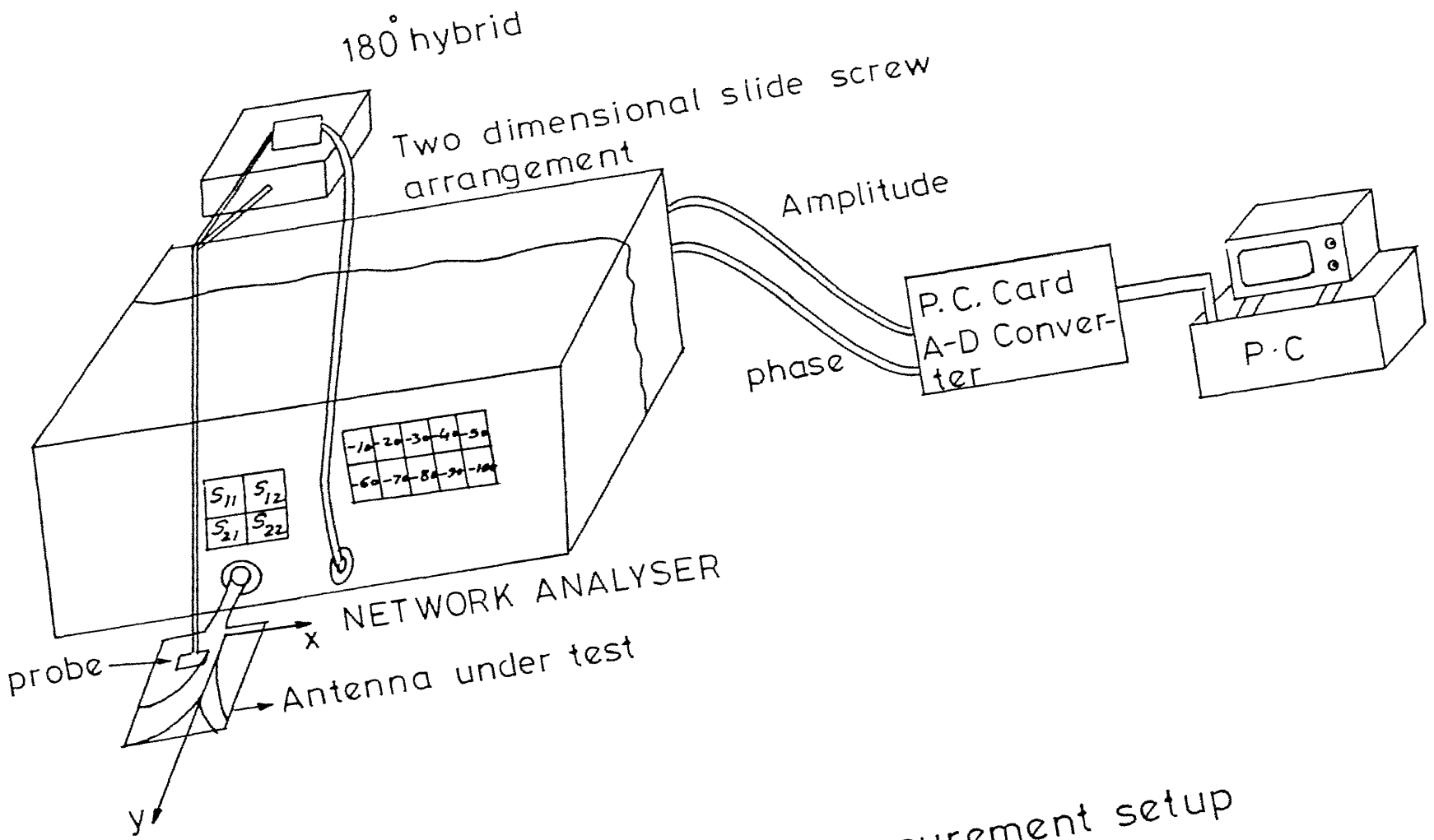


Fig.17 Block diagram of the measurement setup

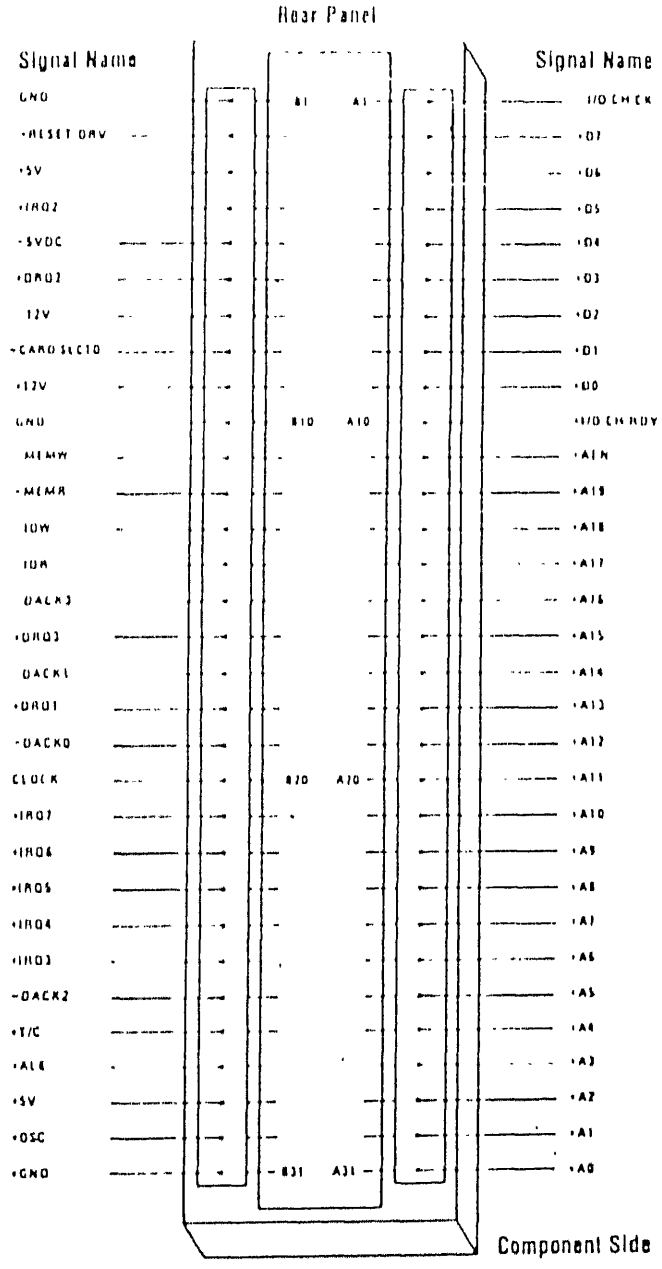


I/O Channel Diagram

1 32-pin slot and its pin configuration

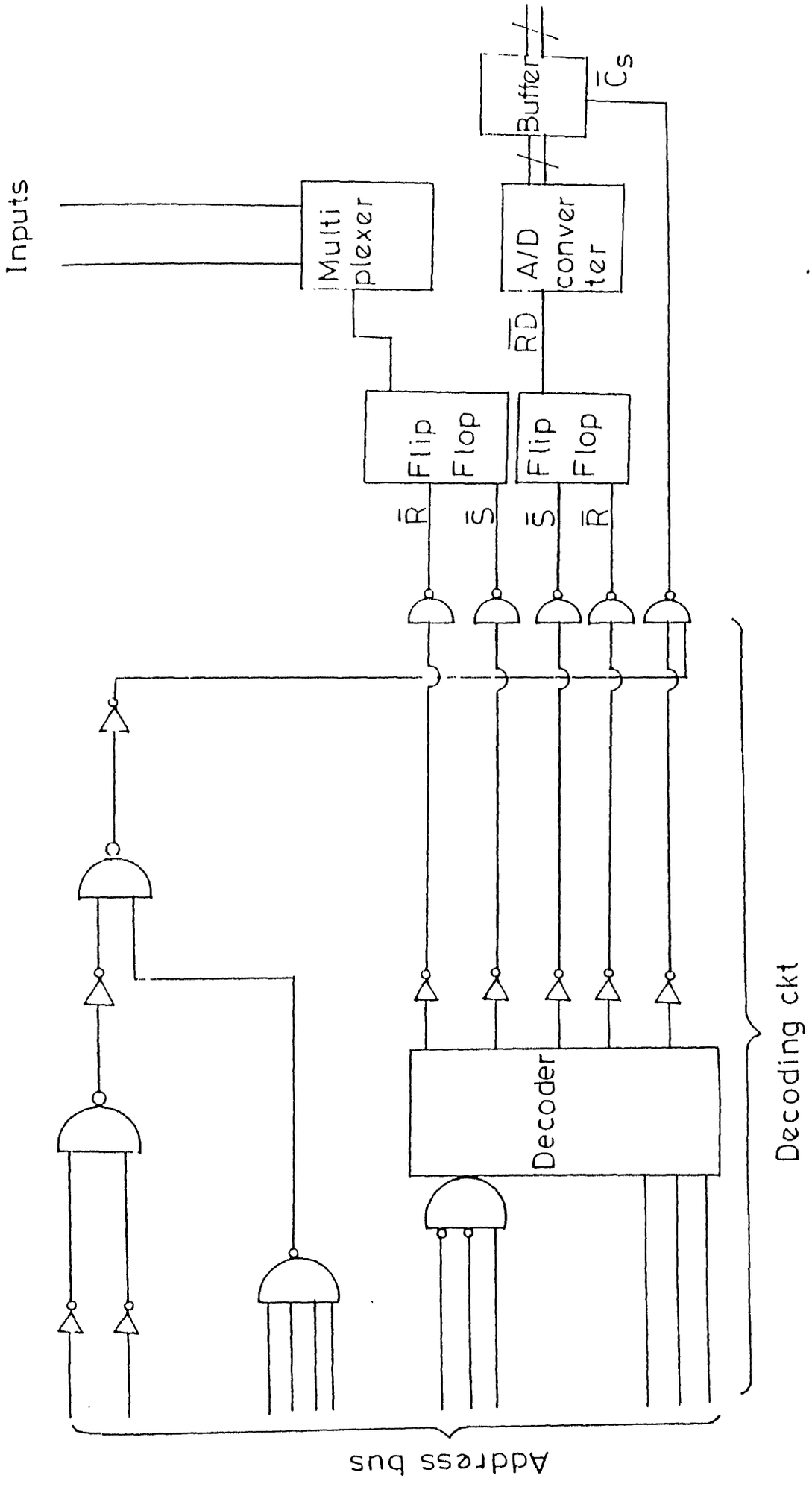


Fig18 Circuit diagram of the A-D Card

control signals, and power and ground lines. All signals on I/o channel are buffered to provide sufficient low-power Schottky (LS) loads per slot.

The 8088 μp is capable of addressing 64 K different ports via its address lines A0 - A15. However a PC system board decodes only lower 10 address lines (A0 - A9) restricting the number of available ports to 1024. The lower half of the 1024 ports are reserved for the system board itself, and the upper half is dedicated to I/o channel. Many of the I/o channel ports are however reserved for the IBM adapter cards. I/o address space 300 - 31 FH allotted to IBM prototype card, are used for present application.

| A9 | A8 | A7 | A6 | A5 | A4 | A3 | A2 | A1 | A0 |
|---|---|---|---|---|---|---|---|---|---|
| 1 | 1 | 0 | 0 | 0 | | | | | |
| always fixed | | | | | bits used for decoding | | | | |

The inclusion of AEN signal for the address decoding is note worthy. This ensures that decoding is not done during DMA cycles. The various chips used are

74LS138 - Decoder

74LS245 - Buffer

4052 - Multiplexer

7574 - A-D converter

The circuit diagram is shown in Figure [18] .

**MEASUREMENT:**

The setup used to measure the current distribution is as shown in Fig. [17]. The input to the antenna is given by port 1

and the received power at port 2 is a direct measure of the tangential magnetic field and hence to the current on the antenna with some proportionality constant.

$$S_{21} \alpha \mid \tan H \mid \alpha \text{ Current density}$$

The probe is held normal to the antenna and is made to move along x-axis for different values of y and along y-axis for different values of x. The orientation of the probe is possible in 2 directions and each direction gives a different component of current. Thus when we have the knowledge of the form of the tangential magnetic field, we have completely characterized the form of the current distribution on the antenna. Since we have information about amplitude and phase of the current distribution, it tells us whether we have a standing wave or travelling wave and also about the nature of decay present.

The data when observed for different values of x for constant y and different values of y for constant x gives us the form of current distribution at that cross section. The graph of phase for a standing wave pattern would be as in Fig.[20] and for travelling wave as in Fig.[20]. Similarly depending on the decay the graph of the amplitude part takes its shape, some of the shapes being given in Fig. [20].

RESULTS AND DISCUSSION:

Measurements have been made at regular intervals of x for constant value of y and for regular intervals of y for constant value of x. The graphs of amplitude and phase variation at

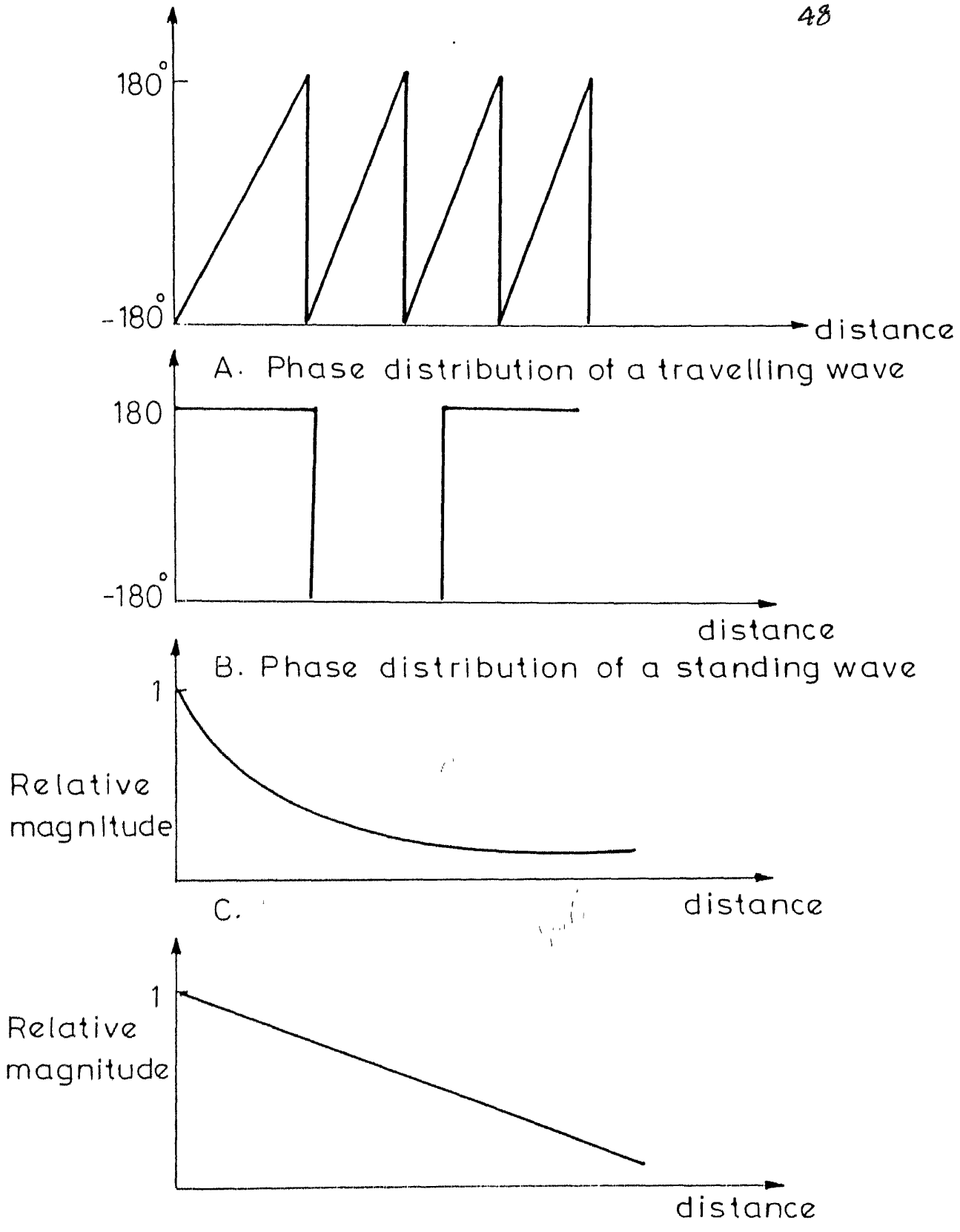


Fig 20 C,D. Amplitude distribution of a decaying wave

different cross sections are given in the Figs. [21] to [24] and the results discussed in the following pages.

The total current distribution J can be split as follows:

$$J = J(x, y) = \hat{x}\, J_x(x, y) + \hat{y}\, J_y(x, y)$$
$$= \hat{x}\, J_x(x) \cdot J_x(y) + \hat{y}\, J_y(x) \cdot J_y(y)$$

In the following pages approximate mathematical forms are given for $J_x(x)$, $J_x(y)$, $J_y(x)$ and $J_y(y)$.

$I_x(x)$

-.-.-.-. phase 50

——— amplitude

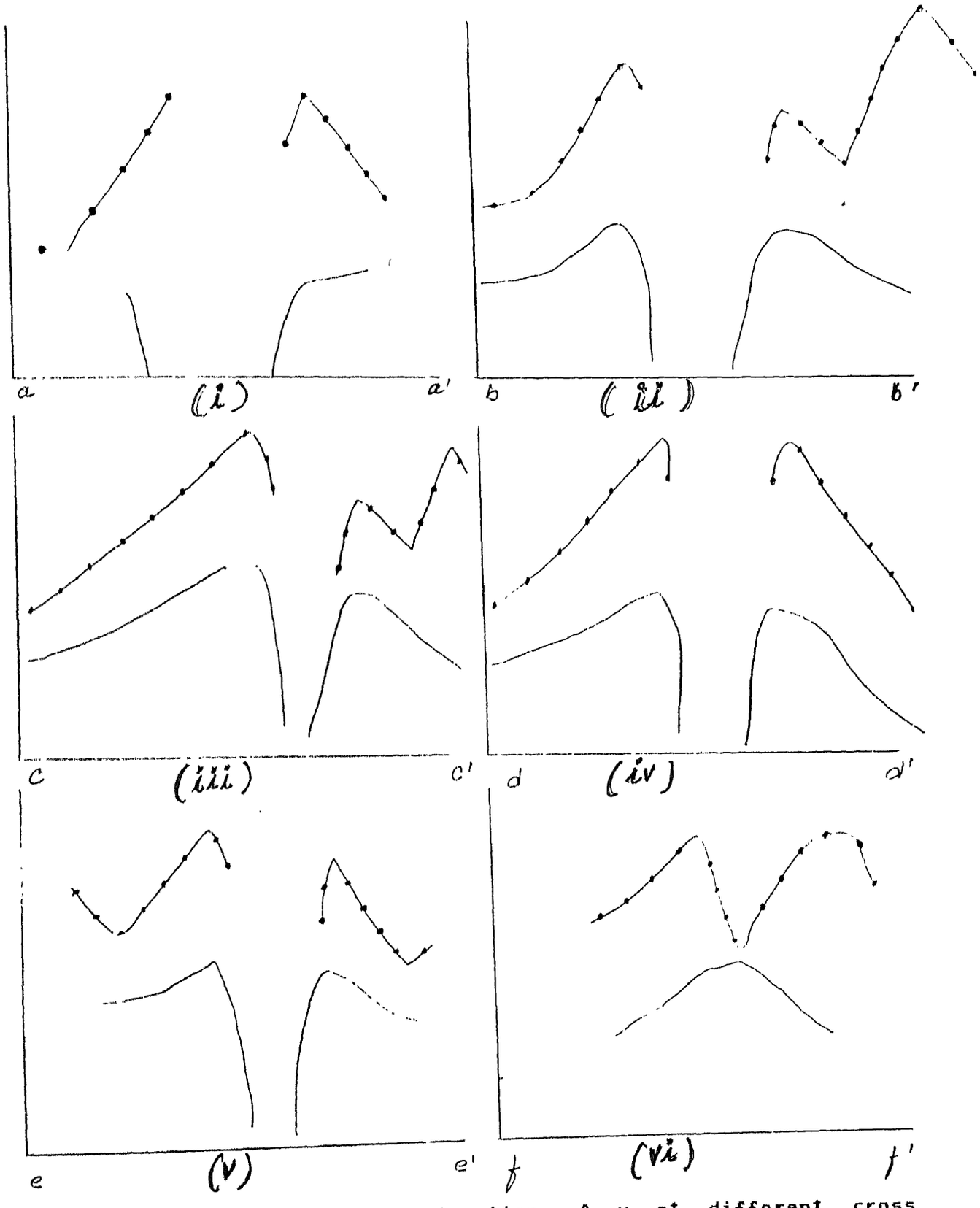


Fig 21. x-directed current as a function of x at different cross sections.

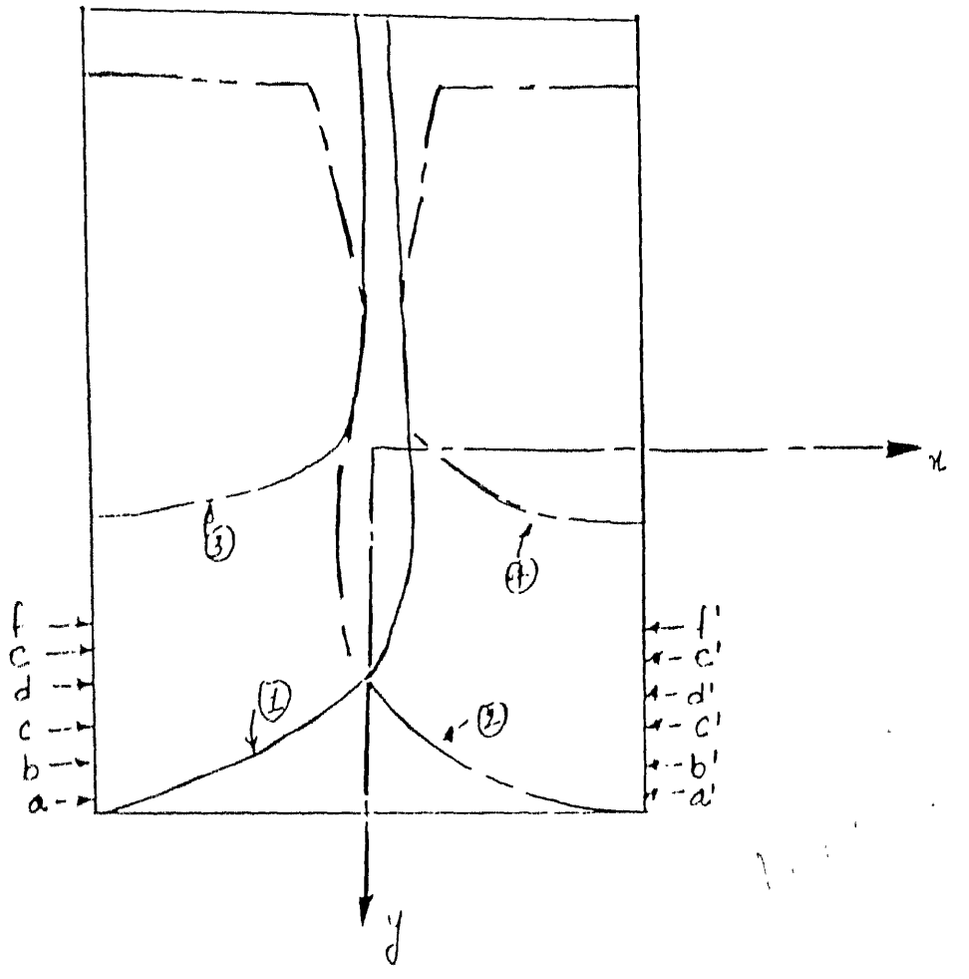


From the plots of the phase at the 6 cross sections it can be seen that the phase has a linear variation with x and hence can be said to have a travelling wave distribution.

From the plots of the amplitude at the 6 cross sections it can be seen that the amplitude decreases as the distance of the observation point is away from the inner curves (1) and (2). Thus we can assume that $J_x(x)$ is a function of x with an attenuation constant and a pohase constant

$$J_x(x) \cong e^{(\alpha_{xx}|x| + j\beta_{xx}x)}$$

where $\alpha_{xx}$ is the attenuation constant and is negative

and $\beta_{xx}$ is the phase constant.

$J_y(x)$



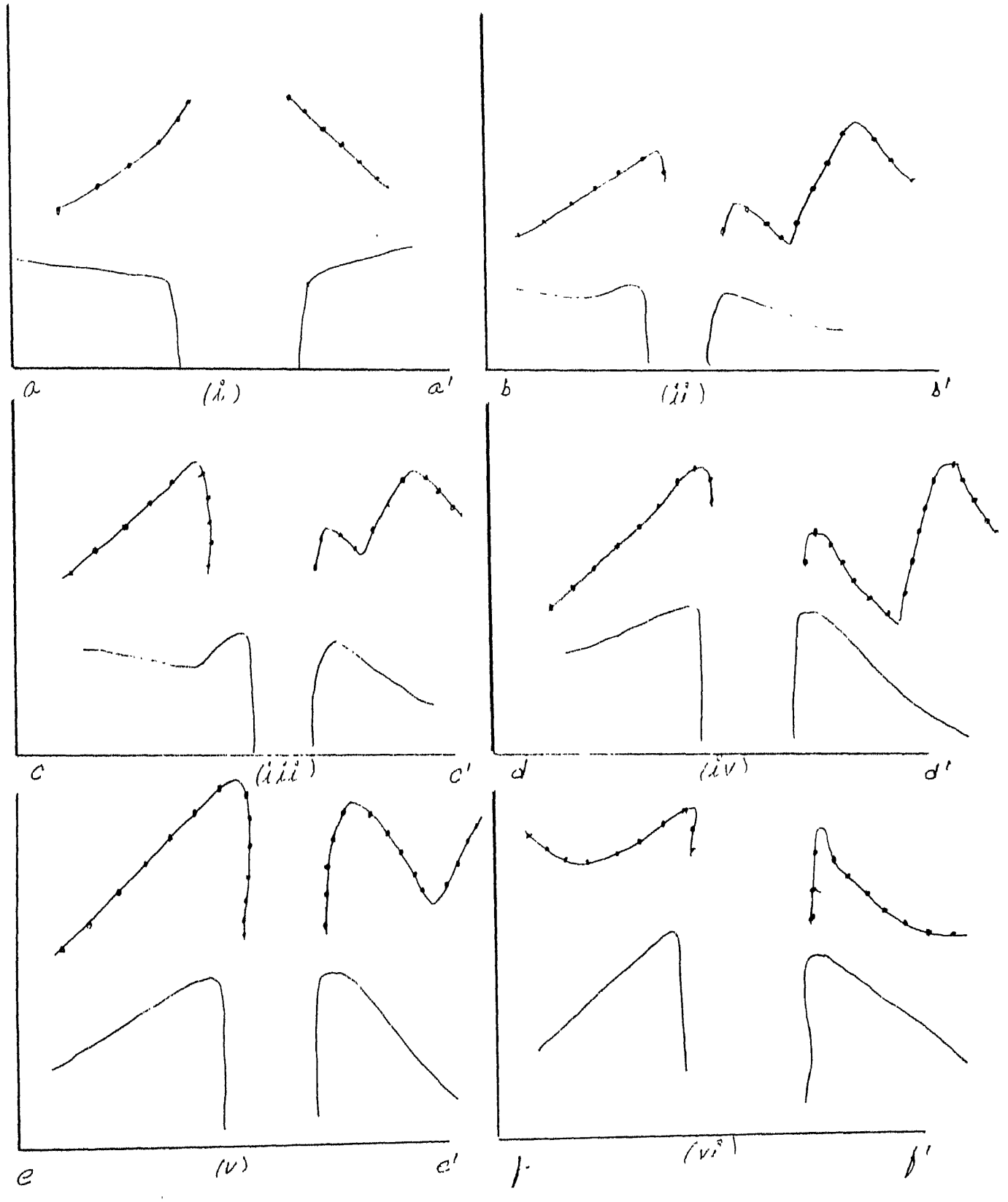


Fig 22 y-directed current as a function of x at different cross sections.

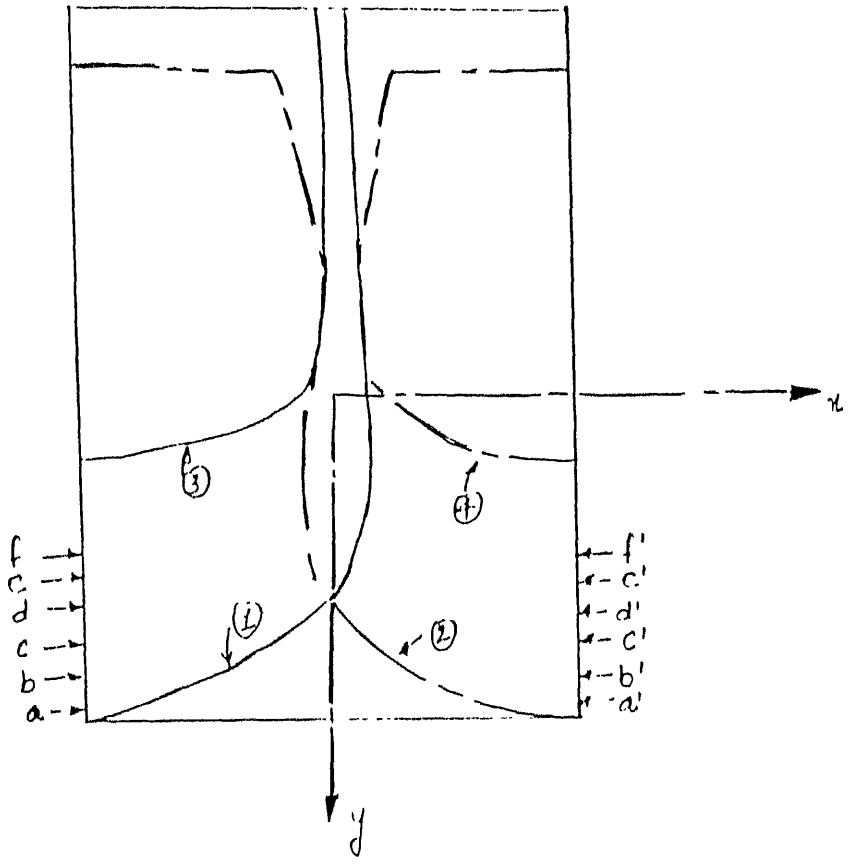


From the phase plot at the 6 cross sections it can be seen that the phase has a linear change and hence a travelling wave.

From the amplitude plots it can be seen that the value of $J_y$ decreases rapidly as we go away outwards of the antenna from the inner curves (1) and (2).

The current distribution $J_y(x)$ can be said to have a form

$$J_y(x) \cong e^{(\alpha_{yx}|x| + \beta_{yx} x)}$$

where $\alpha_{yx}$ is the attenuation constant

$\beta_{yx}$ is the phase constant.

Since the decay is faster $|\alpha_{yx}| > |\alpha_{xx}|$.

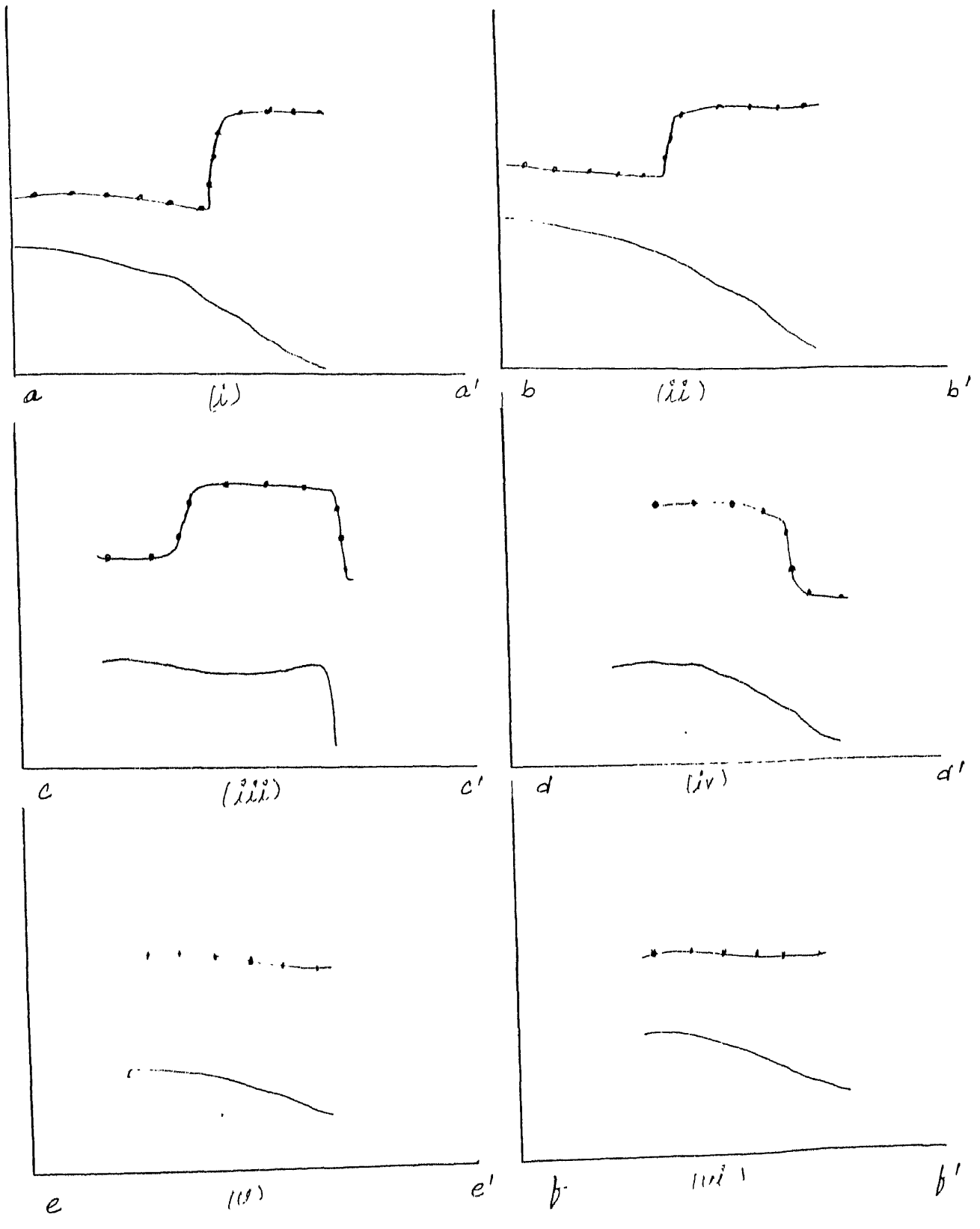


Fig 23 x-directed current as a function of y at different cross sections.

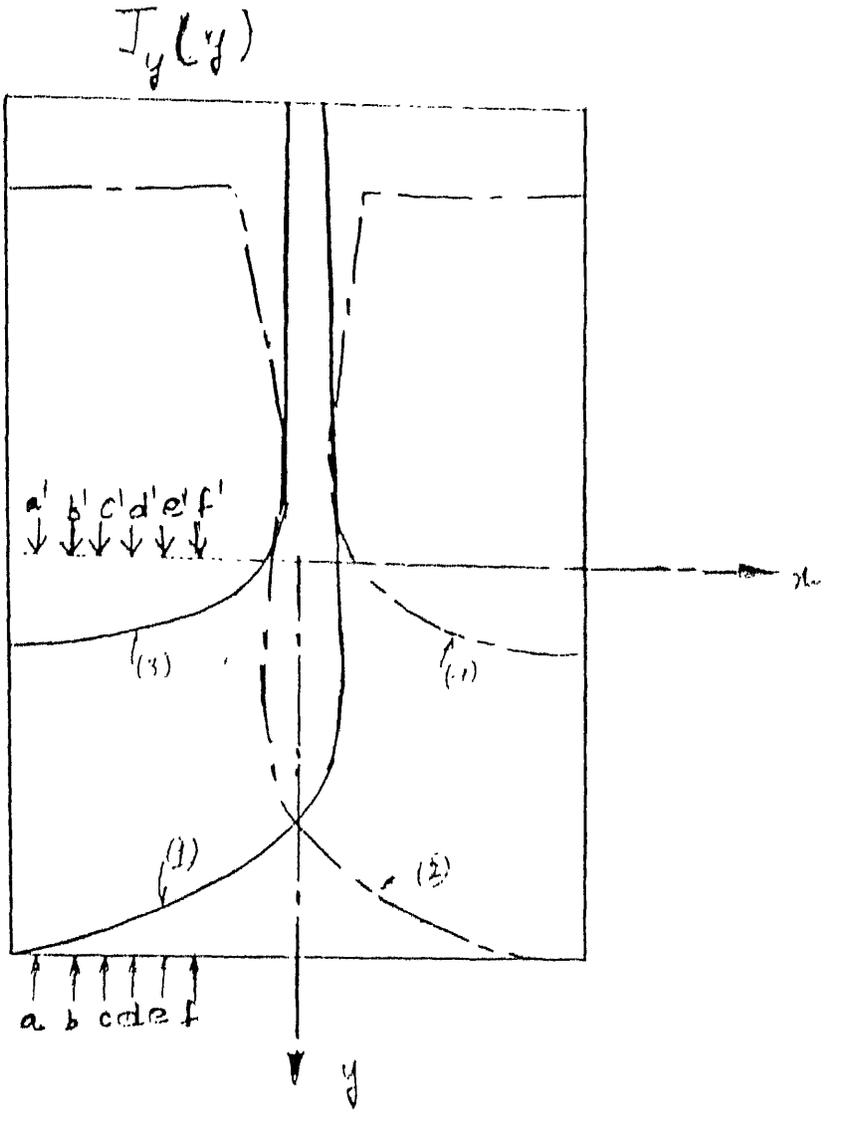


From the plots of phase at the 6 cross section it can be seen that the phase pattern is that of a standing wave pattern.

The amplitude falls rapidly as we go from the inner edges of the antenna (1) and (2) towards the outer edges (3) and (4).

The current distribution $J_x(y)$ can be said to have the form:

$$J_x(y) = e^{(\alpha_{xy}\, y)} \sin(\beta_{xy}\, y)$$

where $\alpha_{xy} > 0$, because amplitude increases as y increases on the antenna surface.

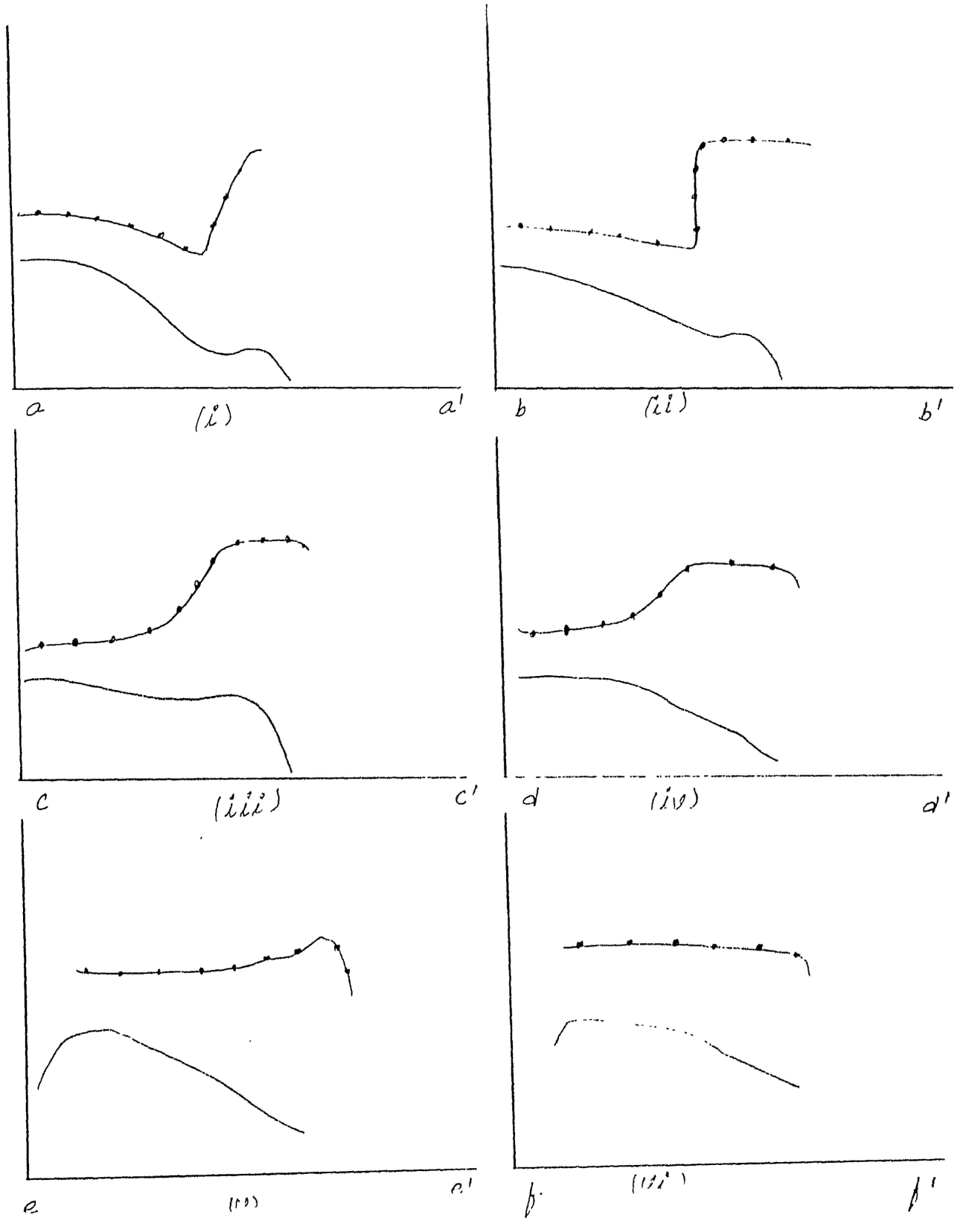


fig 24 y-directed current as a function of y at different cross sections.

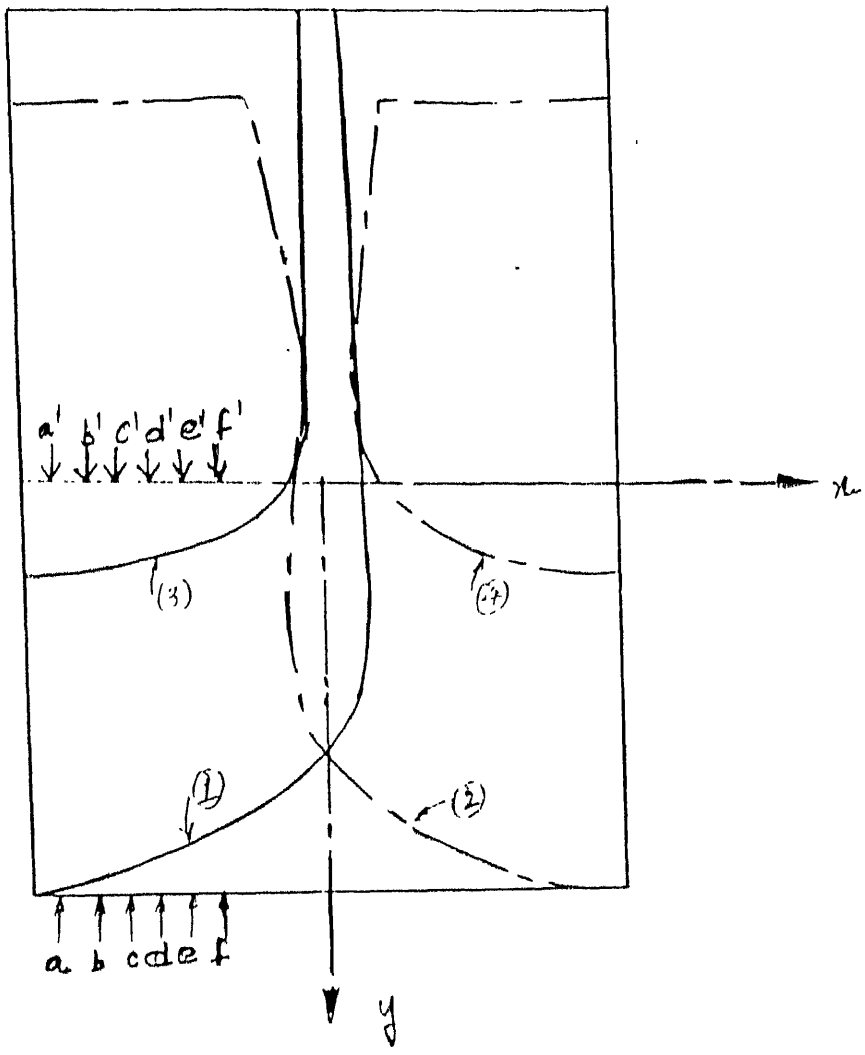


From the plots of phase at the different cross sections it can be observed that $J_y(y)$ has a standing wave patterns.

The amplitude decreases as we go from inner curves of the antenna (1) and (2) towards the outer curves of the antenna (3) and (4). Hence the current distribution $J_y(y)$ can be said to have a form

$$J_y(y) = e^{(\alpha_{yy}\, y)} \sin(\beta_{yy}\, y)$$

where $\alpha_{yy} > 0$.

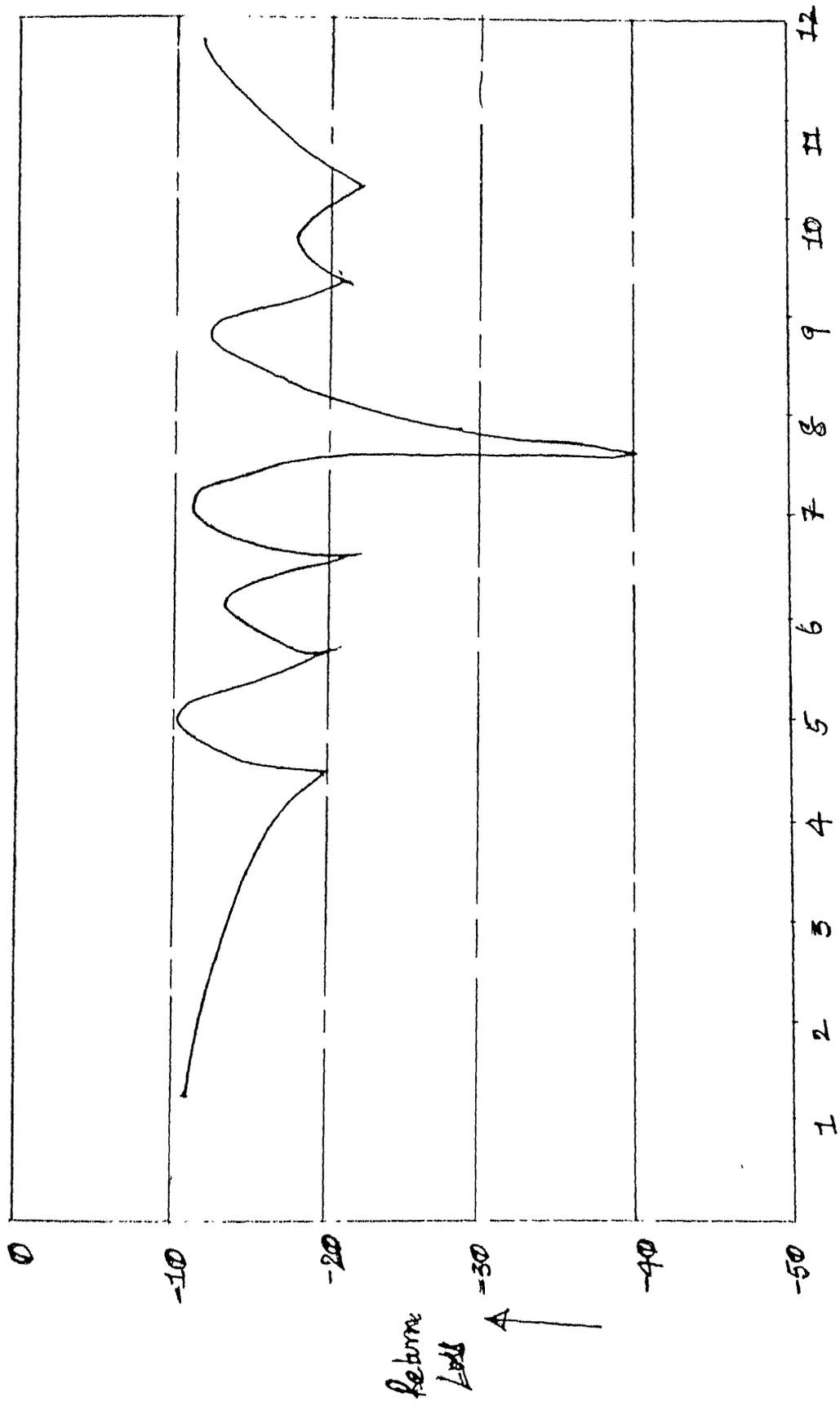


Fig.25 Insertion loss vs. frequency for a vivaldi antenna

The graph of insertion Loss vs. Freq. is given in Fig. [25]. It can be seen that the insertion loss is less than -10 dB for frequencies right from 1 GHz to 12 GHz. Insertion loss of -10 dB implies that 90% of the incident power is radiated and only 10% is reflected due to impedance mismatch. The antenna is resonant at a frequency of 7.4 GHz when it has an insertion loss of around -40 dB, which means that almost all the incident power is radiated.

If dB insertion loss is considered to represent a good antenna then the vivaldi antenna can be seen to have a bandwidth of GHz.

In order to improve the bandwidth and also understand the mechanism of radiation etc., knowledge of current distribution is essential.

# CHAPTER IV

## VIVALDI ANTENNA IN ELLIPTIC CYLINDER COORDINATES

### INTRODUCTION:

It has been observed in the previous chapters that the vivaldi antenna is of a shape, which cannot be solved directly by moment method using rectangular or triangular subdomain basis functions and gross approximations had to be made to solve the antenna. To get results nearer to that of an actual vivaldi antenna, we will try to confine the antenna in a coordinate system which closely approximates the shape of vivaldi antenna in two dimensions. Also since we have got a fairly good idea of the form of current distribution from our measurements, we will use them to get better basis functions.

### ELLIPTIC-CYLINDER COORDINATES [15]:

It is obtained by taking an orthogonal family of confocal ellipses and hyperbolas in a plane and translating in the z-direction Fig.[26]. The coordinate surfaces are elliptic cylinders ($\eta$ = constt), hyperbolic cylinders ($\psi$ = constt) and parallel planes (z = constt). The relation between the new coordinates and rectangular coordinates may be written as

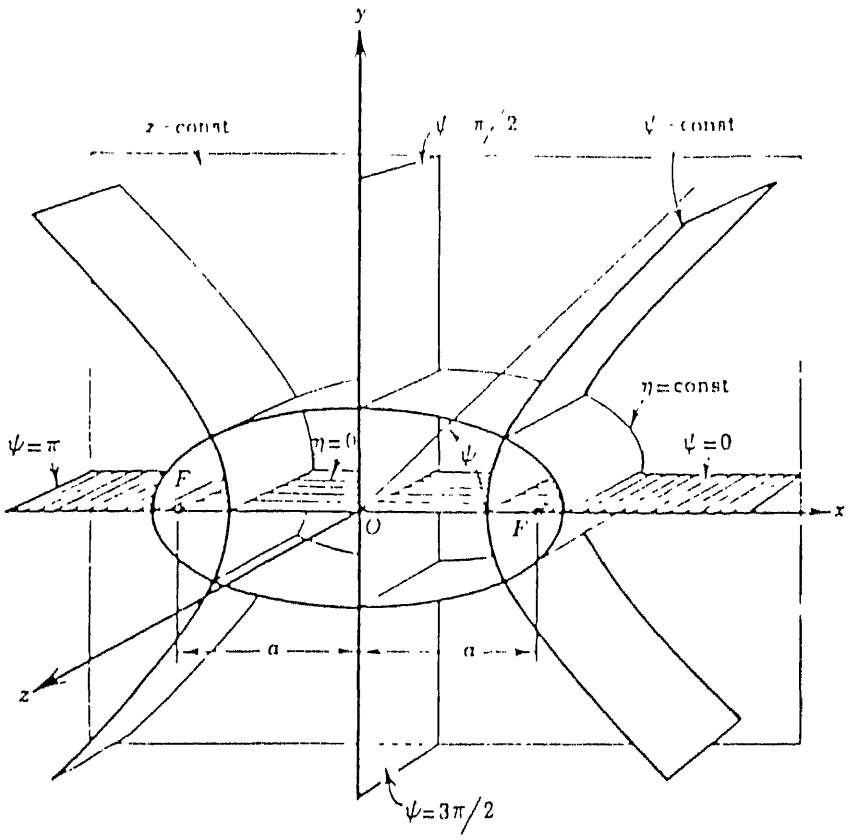


FIG. 26 Elliptic-cylinder coordinates. The coordinate surfaces are elliptic cylinders $\eta$ = const, hyperbolic cylinders $\psi$ = const, and parallel planes $z$ = const.

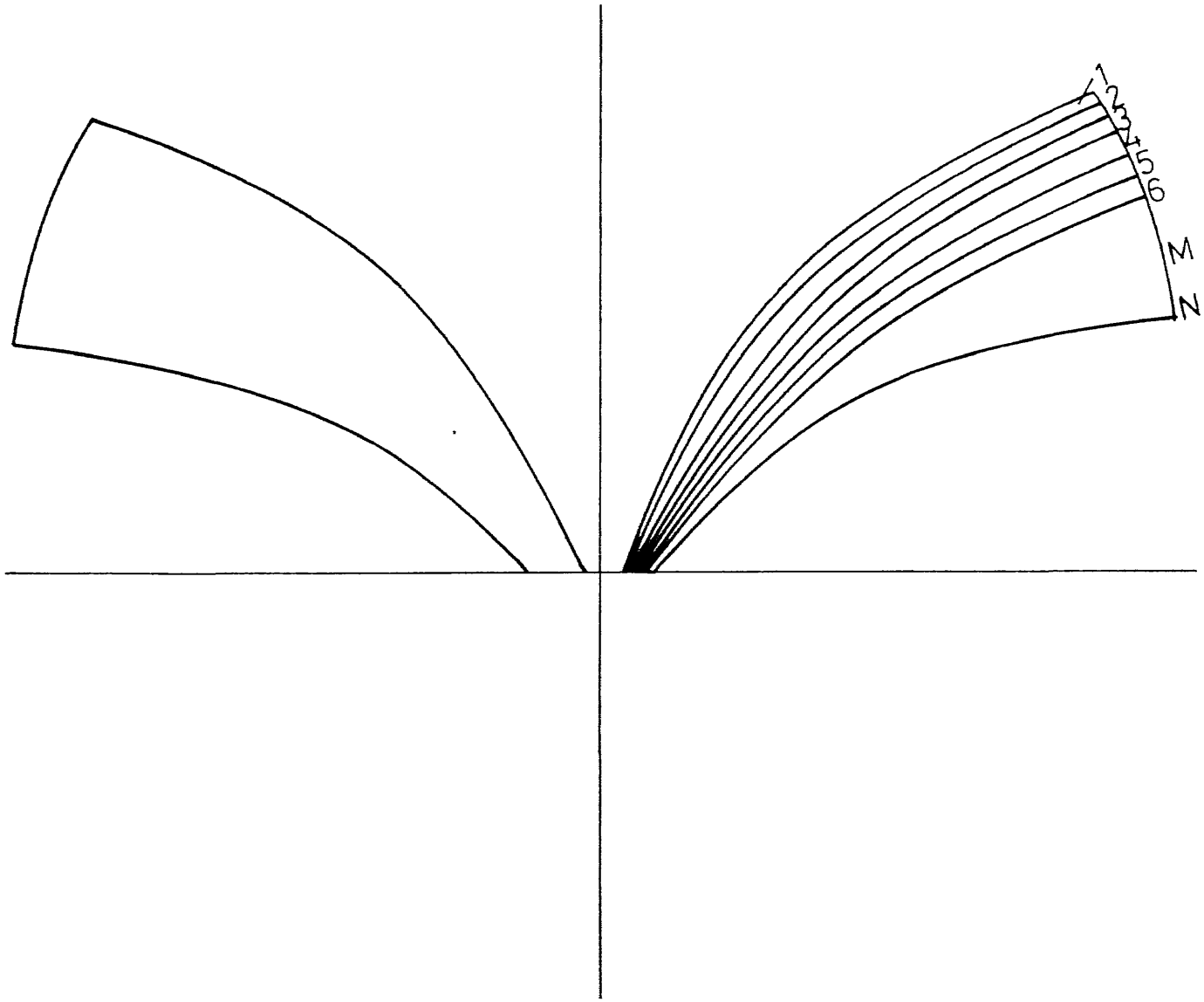


Fig.27 Vivaldi antenna in elliptic cylinder coordinate system

$$x = a \cosh \eta \cos \psi$$

$$y = a \sinh \eta \sin \psi$$

$$z = z$$

The surfaces $\eta$ = constt are elliptic cylinders.

$$\frac{x^2}{(a \cos h\, \eta)^2} + \frac{y^2}{(a \sin h\, \eta)^2} = 1$$

while the surfaces $\psi$ = constt. are the hyperbolic cylinders.

$$\frac{x^2}{(a \cos \eta)^2} + \frac{x^2}{(a \sin \eta)^2} = 1$$

**ENTIRE DOMAIN FUNCTIONS:**

Till now the methods used for solving an antenna for its current distribution always preferred subdomain basis functions, the reason being that the coefficients can then be obtained to match any unknown current distribution, the antenna has. But with the advent of arrays in which thousands of elements are present and especially where the antennas are very close to each other, the time taken to account for all the array element currents and also the mutual impedance effects in addition to the dielectric characterization needs a lot of computation time. Also the use of subdomain basis functions can be better only for antennas which are small in terms of wavelengths.

But once the form of current distribution is known, then use can be made of entire domain functions, which offer various advantages in addition to very less computation time.

Measurements which were made on vivaldi antenna gave the current distribution which was explained in the previous chapter. From the graphs it can be observed that the current distribution followed a particular pattern when we try to analyse the vivaldi antenna in the elliptic cylinder coordinate system, we need to have the basis functions in the two orthogonal directions $\hat{a}_{\eta}$ and $\hat{a}_{\psi}$.

We can see from the diagram below that the $\eta$ current which enters at the input tends to more along the curved path of the antenna and a rough approximation would be to assume that for $\psi$ = constt. the current has a travelling wave distribution with a decay which accounts for the radiation field.

It can also be seen that $\eta$ current has standing wave distribution for $\eta$ = constt berause it can be approximated as a wave front of equal phase.

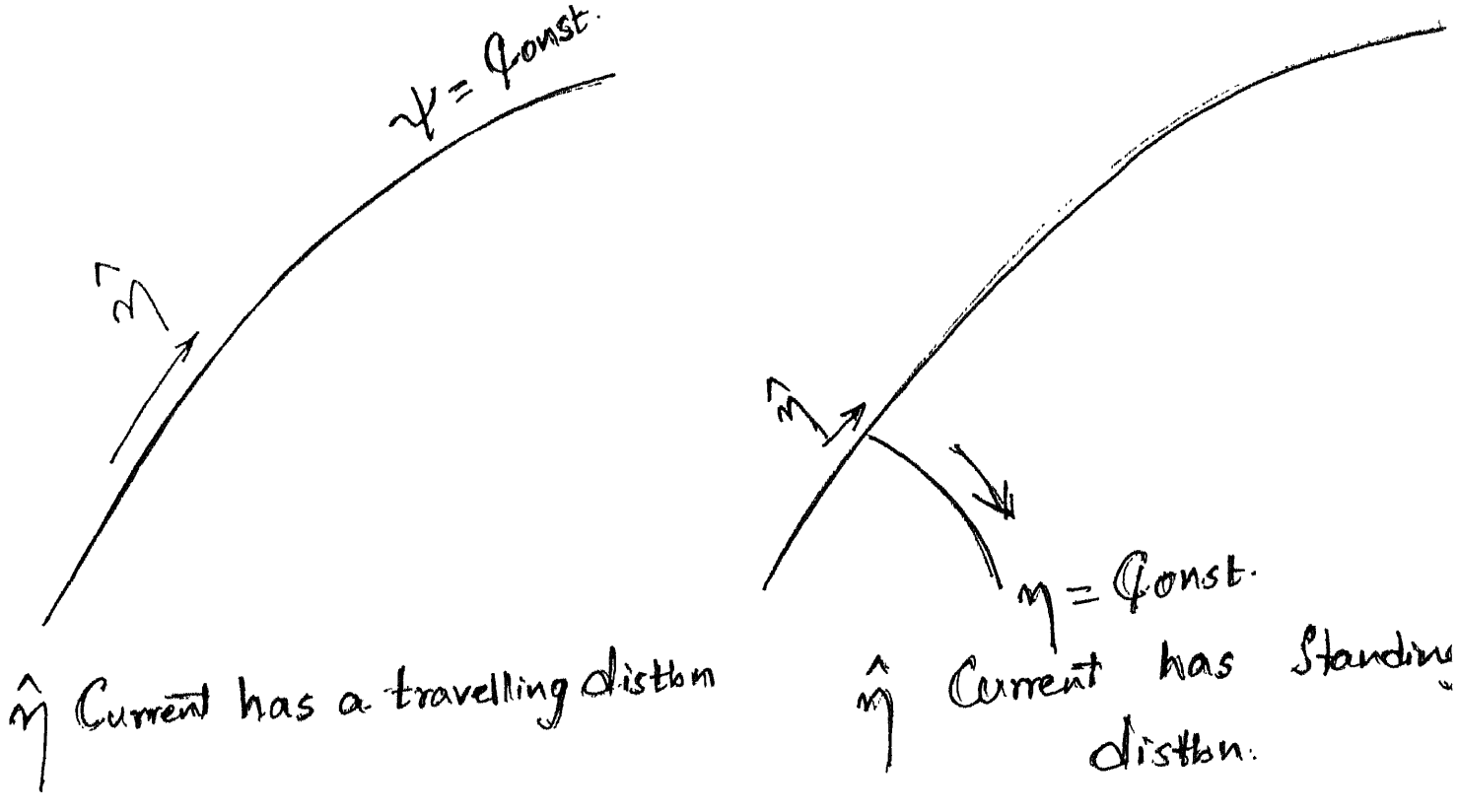

Similarly $\hat{\psi}$ current has travelling distribution with fast decay for $\psi$ = constt as seen from diagram below and $\hat{\psi}$ current has standing distributin with a little decay for $\eta$ = constant.

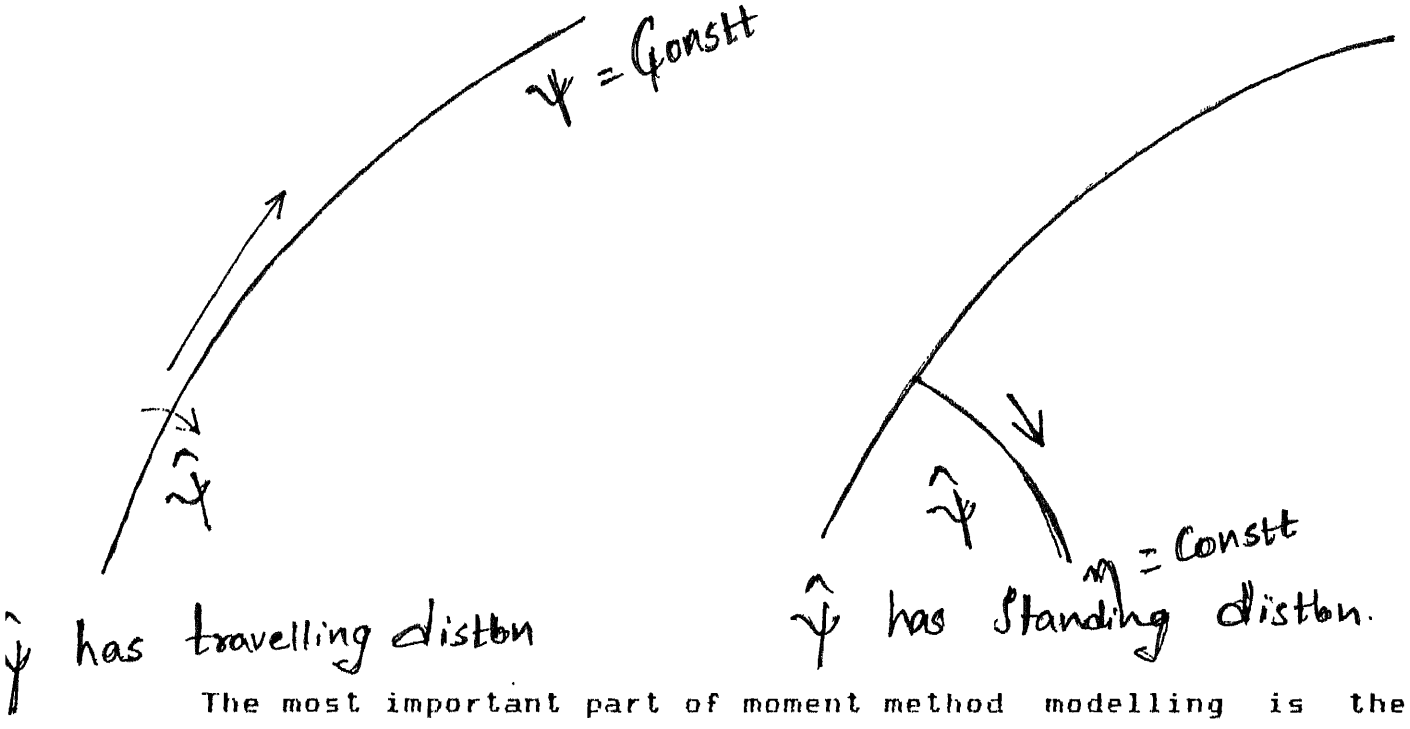


The most important part of moment method modelling is the evaluation of impedance elements of the impedance matrix which are the reactions between the two elements

$$Z_{mn} = -\int \bar{J}_n . \bar{E}_m \, dS$$

where $Z_{mn}$ is the mutual impedance between the m-th testing mode and n-th expansion mode.

The right hand side matrix elements [V] are given by

$$V_m = \iiint_V (\bar{J}_i . \bar{E}_m - \bar{M}_i . \bar{H}_m) \, dv$$

where $(\bar{J}_i, \bar{M}_i)$ are the excitations and $(\bar{E}_m, \bar{H}_m)$ are the fields at the excitation point due to the m-th test source.

Our experimental results also show a similar behaviour. The above analysis then allow us to assume entire domain functions which have the mathematical form:

$$\bar{J} = \hat{\eta}\, J_{\eta}(\eta, \psi) + \hat{\psi}\, J_{\psi}(\eta, \psi)$$

$$\hat{\eta}\, J_{\eta}(\eta).\, J_{\eta}(\psi) + \hat{\psi}\, J_{\psi}(\eta).\, J_{\psi}(\psi)$$

where $J_{\eta}(\eta)$, $J_{\eta}(\psi)$, $J_{\psi}(\eta)$, $J_{\psi}(\psi)$ has the forms as was just explained, with attenuation constant accounting for the decay and phase constant accounting for the phase transition.

In order to solve for the current distribution on the vivaldi antenna, we divide our antenna into a number of subsections as shown in Fig.[27], on which we assume only $\hat{\eta}$ directed current distribution for simplicity and assume that on each strip it is constant in the $\psi$ direction.

For finding the impedance elements we need to have expressions for near field in the elliptic-cylinder coordinate systems.

EXPRESSION FOR NEAR-FIELD-EVALUATION:

If we assume that only $\hat{\eta}$ directed current is present and it is of the form

$$I = \hat{\eta}\, c\, e^{(\alpha+j\beta)\,\eta'} \quad \{ \text{assuming } f(\psi') = \text{constant} \}$$

$$\bar{A} = \frac{\mu}{4\pi} \int \hat{\eta}\, c\, e^{(\alpha+j\beta)\,\eta'} \frac{e^{-j\beta R}}{R}\, d\eta'$$

$$= \frac{\mu}{4\pi} \int \left( \frac{e^{-j\beta R}}{R} \right) \hat{\eta}\, f(\eta', \psi', z')\, d\eta'.$$

$$H = \frac{1}{\mu} \nabla \times \bar{A} = \frac{1}{4\pi} \nabla \times \int \left( \frac{e^{-j\beta R}}{R} \right) \hat{\eta}\, f(\eta', \psi', z')\, d\eta'$$

$$= \frac{1}{4\pi} \int \nabla \times \left\{ \left( \frac{e^{-j\beta R}}{R} \right) \hat{\eta} \, f(\eta', \psi', z') \right\} d\eta'$$

$$\nabla \times (g\bar{F}) = (\nabla g) \times \bar{F} - g(\nabla \times \bar{F})$$

$$\bar{H} = \frac{1}{4\pi} \int \nabla \left( \frac{e^{-j\beta R}}{R} \right) \times \hat{\eta} \, f(\eta', \psi', z') \, d\eta'$$

$$= \frac{1}{4\pi} \int \left\{ -\hat{R} \left( \frac{1+j\beta R}{R^2} \right) e^{-j\beta R} \right\} \times \left\{ \hat{\eta} \, f(\eta', \psi', z') \right\} d\eta'$$

The expression for relation between unit vectors in elliptic-cylinder coordinates and cylinder coordinates is given in Appendix 1).

$$\bar{H} = \frac{1}{4\pi} \int - \left[ \hat{i} (x - x') + \hat{j} (y-y') + \hat{k} (z-z') \right]$$

$$\left( \frac{1+j\beta R}{R^2} \right) e^{-j\beta R} \times \left( \frac{1}{(g_{11})^{1/2}} \left[ \hat{i} \cosh \eta' \sin \psi' \right. \right.$$

$$\left. \left. + \hat{j} \sinh \eta' \cos \psi' \right] \right) f \left\{ \blacksquare \, \blacksquare \, (\eta', \psi', z') \right\} d\eta'$$

$$= \frac{1}{4\pi} \int \frac{1}{(g_{11})^{1/2}} \left[ \hat{k} (x-x') \sinh \eta' \cos \psi' \right.$$

$$-\hat{k} (y-y') \cosh \eta' \sin \psi' - \hat{i} (z-z') \sinh \eta' \cos \psi'$$

$$\left. \hat{j} (z-z') \cosh \eta' \sin \psi' \right] e^{-j\beta R} \left( \frac{1+j\beta R}{R^2} \right)$$

$$f \left\{ \blacksquare \, \blacksquare \, (\eta', \psi', z') \right\} d\eta'$$

It has 4 components. Consider only 1 component $\hat{i}$

$$\bar{E} = -\frac{1}{j \omega \in} \nabla \times \bar{H}$$

$$= \frac{1}{4\pi\ j\ \omega\ \epsilon} \nabla \times \int g\ \bar{F}\ d\eta'$$

$$= \frac{1}{j\ 4\pi\ \omega\ \epsilon} \nabla \times \int - \hat{i}\ (z-z')\ \sinh\eta'\ \cos\psi'\ \frac{1}{(g_{11})^{1/2}}$$

$$e^{-j\beta R} \left[ \frac{1+j\beta R}{R^2} \right] f \left\{ \spadesuit\ \spadesuit\ (\eta', \psi', z') \right\} d\eta'$$

Again using the identity

$$\nabla \times (g\ \bar{F}) = (\nabla\ g) \times \bar{F} - g(\nabla \times \bar{F})$$

we can expand the above expression. Similarly for the other 3 components.

Finally on simplification we get an expression of the form

$$\bar{E} = \int (\hat{a}_\eta\ U_1 + \hat{a}_\psi\ U_2 + \hat{a}_z\ U_3)\ d\eta'$$

where

$$U = f \left\{ \eta', \psi', z', \eta, \psi, z \right\}$$

Since we now have a single integration formula for calculating $\bar{E}$ field we can get the impedance elements

$$Z_{mn} = - \int \bar{E}_m \cdot \bar{J}_n\ ds$$

and thus we can fill the impedance matrix. We can then find the current distribution by inverting the matrix and multiplying it by excitation vector.

$$[I] = [Z]^{-1}\ [V]$$

where $[I]$ = unknown vector

$[Z]$ = impedance matrix

$[V]$ = excitation matrix

As a convenient check it can be used to find the current distribution at the input point where it should have a form similar to that of a assymetric slot line

Since the antenna is solved in its natural coordinate system we get a better feel of the current distribution and also of the radiation mechanism. Also the computation time will be decreased because of the use of entire domain functions, because of which various antennas with different $\eta_1$, $\eta_2$, $\psi_1$, $\psi_2$ limits can be evaluated for their bandwidth and other properties. This idea can be extended to the numerous antennas which are confined to the different coordinate systems like using sinusoidal patch dipoles for rectangular antennas.

# CHAPTER V

# SUMMARY, CONCLUSIONS AND SCOPE FOR FURTHER WORK

## SUMMARY AND CONCLUSIONS:

In this thesis an exponentially tapered slot antenna known as vivaldi antenna is analysed. The antenna is fabricated on a low dielectric substrate. This antenna is different from other microstrip printed antennas. The usually present ground plane and a resonant cavity between the top surface and the ground plane are absent. The antenna is a tapered transmission line which radiates as the slot width increases. The taper is extended over a length of $\lambda/2$, thus realizing a large bandwidth. Also the transition from microstrip line to the antenna is made over a length of $\lambda/2$. The antennas insertion loss characteristics were measured and found to show a large bandwidth.

The most widely used moment method to solve the integral equation is discussed and applied to a dipole antenna and a microstrip patch antenna. The advantages of entire domain functions and the significance of the source modelling are discussed. The knowledge of exact current distribution is found to be necessary for finding out the near field and also the

radiation pattern and input impedance. Input impedance is found to be sensitive to the way we model the source.

In order to obtain a good idea about the form of current distribution, measurements of the near field are done. The forms obtained are discussed. Finally the antenna is confined to an elliptic cylinder coordinate system and is divided into subdomains on which current can be assumed with the help of the measured patterns. Since the antenna is solved in a coordinate system in which it confines to some orthogonal surfaces it can lead to better results.

SCOPE FOR FURTHER WORK:

Further theoretical work needed are the programming of the proposed method for various valves of $\eta$'s and $\psi$'s and the evaluation of the bandwidth for these antennas. Study of the transition from microstrip to assymetric slot line and minimisation of the length of the transition are also important.

Mutual coupling behaviour has to be formulated to study the performance of elements in array environment. This is very important because at spacings small compared to wavelength, the mutual coupling is very strong and will determine the input impedance behaviour with frequency.

Finally the design of a circular array of such antennas with a radial power divides [16] and combines to get the desired omnidirectional power pattern can be carried out.

# REFERENCES


1. John Q. Howell, "Microstrip Antennas", IEEE Transactions on Ant & Propogation, pp. 90, Jan. 1975.

2. P.J. Gibson, "The Vivaldi Aerial", Proc. 9th European Microwave Conference, Brighton, U.K. 1979, pp. 120-134.

3. S. Mahapatra and S.N. Prasad, "A new MIC Slot Line Aerial", Proc. 9th European Microwave Conference, Brighton, U.K., 1979, pp. 101-105.

4. R.K. Janaswamy and Daniel H. Schavbert, "Analysis of the Tapered Slot Antenna", IEEE Transactions on A & P, Sept. 1987, pp. 1058.

5. R.K. Janaswamy, "An Accurate moment method model for the tapered slot antenna", IEEE Transactions on A & P, Dec. 1989, pp. 1523.

6. Ehod Gazit, "Improved Design of the Vivaldi Antenna", IEEE Proceedings, April 1988, p. 89.

7. Jordan and Balmain, "Electromagnetic Waves and Radiating Systems", Prentice Hall of India Pvt. Ltd.

8. John D. Dyson, "Measurement of Near Fields of Antennas and Scatterers", IEEE Trans. on A & P, July 1973, p. 446.

9. IBM P.C. User Manual and Technical Reference.

10. Constantine A. Balanis, "Advanced Engineering Electromagnetics", John Wiley & Sons.

11. Edward H. Newman and Pravit Tulyathan, "Analysis of Microstrip Antennas Using Moment Methods", IEEE Trans. on A & P, January 1981, p. 47.

12. V.H. Rumsey, "Reaction Concept in Electromagnetic Theory", Physical Review, June 15, 1954, p. 1483.

13. Jack H. Richmond, "Rigorous Near zone Field Expressions for Rectangular Sinusoidal Surface Monopole", IEEE Trans. on A & P, May 1978, pp. 509.

14. N.N. Wang, Jack H. Richmond, "Sinusoidal Reaction Formulation for Radiation and Scattering from Conducting Surfaces", IEEE Trans. on A & P. May, 1975, p. 376.

15. Moon and Spencer, "Field Theory for Engineers", The Van Nostrand Series in Electronics and Communications.

16. A. Fathy and D. Kalokitis, "Analysis and Design of a 30-way Radial Combiner for KU-band Applications", RCA Review, Vol. 47, Dec. 1986, pp. 487.

# APPENDIX 1

## RELATION BETWEEN THE UNIT VECTORS OF ELLIPTIC - CYLINDER AND RECTANGULAR COORDINATES

The conversion of a vector from one coordinate system to another coordinate system requires the knowledge of the relationship of the unit vectors of the coordinate systems. The unit vector $\hat{i}$ is perpendicular to the surface $n$ = constt and similarily $\hat{\eta}$ is perpendicular to $\eta$ = constt. The combining relation between the 2 coordinate systems is

$$x = a \cosh \eta \cos \psi$$

$$y = a \sinh \eta \sin \psi$$

$$\nabla x = \hat{i} \frac{\partial}{\partial x} (x) = \hat{i}$$

$$\nabla (a \cosh \eta \cos \psi) = \frac{\hat{a}_\eta}{(g_{11})^{1/2}} \frac{\partial}{\partial \eta} (a \cosh \eta \cos \psi) + \frac{\hat{a}_\psi}{(g_{11})^{1/2}} \frac{\partial}{\partial \psi} (a \cosh \eta \cos \psi)$$

where $g_{11} = g_{22} =$

hence $$\hat{i} = \frac{\hat{a}_\eta}{(g_{11})^{1/2}} \frac{\partial}{\partial \eta} (a \cosh \eta \cos \psi) + \frac{\hat{a}_\psi}{(g_{11})^{1/2}} \frac{\partial}{\partial \psi} (a \cosh \eta \cos \psi)$$

Similarly,

$$\hat{j} = \frac{\hat{a}_\eta}{(g_{11})^{1/2}} (a \cosh \eta \cos \psi) + \frac{\hat{a}_\psi}{(g_{22})^{1/2}} (a \sinh \eta \cos \psi)$$

Solving equations (1) and (2) we get,

$$\hat{i} = \frac{1}{(g_{11})^{1/2}} \left[ \hat{a}_\eta (a \sinh \eta \cos \psi) + \hat{a}_\psi (-a \cosh \eta \sin \psi) \right.$$

and $$\hat{j} = \frac{1}{(g_{11})^{1/2}} \left[ \hat{a}_\eta (a \cosh \eta \sin \psi) + \hat{a}_\psi (a \sinh \eta \cos \psi) \right]$$

$$\hat{k} = \hat{a}_z .$$

# APPENDIX 2

## SOFTWARE FOR DATA ACQUISITION

```
Program atd;

Uses dos, crt;

Const

     ad-amp = $0318
     ad-phase = $0319
     ad-rd-low = $031A
     ad-rd-high = $0318
     ad-cs = $031C
     zero = $00
     ESc = # 27

Type

     DataArray = array [0..501] of byte;
     VoltArray = array [0..501] of longint;

Var

     outfile : text;
     hour,min,sec,sec100:word;
     port-Addr,I,J, channel:integer;
     dummy:byte;
     ch:char;
     Amp,phase:Dataarray
     Volt:Voltarray

Function Sample -ATD (port-Addr:integer): byte;

Var

     dummy:byte
```

```
begin

      dummy:= port [port-Addr]
      dummy:= port [ad-rd-low]
      dummy:= port [ad-rd-high]
      delay (1)
      dummy:= port [ad-rd-low]
      delay (1)
      sample-ATD:= port [ad-cs]
end;

Begin

      Writeln ('A to D')
      writeln; writeln;
      ch:= ' '; I:= 0;
      gettime (hour, min, sec, sec100);
      Writeln ('time:' hour:3, min::3, sec: 3, sec100:3);
      Writeln ('To start press key');
      ch:=readkey;

      Repeat

            I:=I+1
            Write
            ('Voltage=');
            Volt(i):=i;
            Amp[1]:=sample-ATD (Ad-Amp);
            phase [I]:= sample-ATD (Ad-phase);
            Writeln ('Amp:=', Amp[1], 'phase:', phase [1]:6);
            Writeln;
            Writeln ('press any key (ESc to end)';
            Writeln;
            ch:=readkey;

      Until ch=ESc;
      assign (outfile, 'Data out');
      rewrite (outfile);
      Writeln (outfile, 'x-axis (mm)      phase     Amplitude');
      for j:=1 to i do
      Writeln (outfile, volt[J]:6', '     ', Amp[J]: 6, phae [J]:6);
      Writeln (outfile 'Go to lotus')
      close (outfile)
      end.
```